12-2007

Virtual Modeling and Verification of Air-Ride Truck Seat using Multibody Dynamics for Whole Body Vibration Evaluation

Devdutt Nandkishore Shende
University of Tennessee - Knoxville

To the Graduate Council:

I am submitting herewith a thesis written by Devdutt Nandkishore Shende entitled "Virtual Modeling and Verification of Air-Ride Truck Seat using Multibody Dynamics for Whole Body Vibration Evaluation." I have examined the final electronic copy of this thesis for form and content and recommend that it be accepted in partial fulfillment of the requirements for the degree of Master of Science, with a major in Mechanical Engineering.

Jack Wasserman, Major Professor

We have read this thesis and recommend its acceptance:

J. A. M. Boulet, John D. Landes

Accepted for the Council:
Carolyn R. Hodges

Vice Provost and Dean of the Graduate School

(Original signatures are on file with official student records.)

To the Graduate Council:

I am submitting herewith a thesis written by Devdutt Nandkishore Shende entitled "Virtual Modeling and Verification of Air-Ride Truck Seat using Multibody Dynamics for Whole Body Vibration Evaluation". I have examined the final electronic copy of this thesis for form and content and recommend that it be accepted in partial fulfillment of the requirements for the degree of Master of Science, with a major in Mechanical Engineering.

Jack Wasserman

Major Professor

We have read this thesis
and recommend its acceptance:

J. A. M. Boulet

John D. Landes

Accepted for the Council:

Carolyn R. Hodges

Vice Provost and
Dean of the Graduate School

(Original signatures are on file with official student records.)

Virtual Modeling and Verification of Air-Ride Truck Seat using Multibody Dynamics for Whole Body Vibration Evaluation

A Thesis

Presented for the

Master of Science

Degree

The University of Tennessee, Knoxville

Devdutt Nandkishore Shende

December 2007

Dedication

I dedicate this thesis to my parents Nandkishore and Manik Shende for their trust, support and encouragement without which my success in this program would not have been possible.

Acknowledgements

I wish to thank my advisor, Dr. Jack Wasserman for his guidance and knowledge during the course of my graduate studies at the University of Tennessee. I am grateful to him for providing me the financial support and this research opportunity without which, my Master's program would not have been such a great learning experience. I also would like extend my thanks to the thesis committee members, Dr. J. A. M. Boulet and John D. Landes for their guidance, review and suggestions.

I also would like to thank Logan Mullinix and Kelly Neal of Commercial Vehicle Group for allowing me the access to their test facility at National Seating and also for funding the study. Logan Mullinix and Dr. Jack Wasserman were the technical minds behind the conception of this project. Kelly Neal was always available for help with logistics, testing, data collection and coordination with National Seating's test lab. Sampath Kandala, the testing engineer at National Seating, was of immense help in setting up the seat and simulator tests. I am extremely grateful to him for taking time out of his busy schedule and helping me with this study. His invaluable suggestions and testing expertise are greatly appreciated. This research would not have been possible without the support form Commercial Vehicle group and National Seating.

Abstract

To aid the tuning and optimization of the truck seat design to specific trucks and road profiles during the design phase, this study presents the development and validation of a virtual seat model. This study also assess the utility of the model for whole body vibrations evaluation.

The virtual dynamic seat model was developed in MSC. ADAMS/VIEW. The critical elements like the suspension mechanism, the airspring, dampers and seat cushion were modeled using tested data. To validate the performance of the virtual model, prototype tests were performed using the MTS 6-axis simulator. The modeling process was targeted to achieve a good correlation between measured and simulated data around the 5Hz frequency zone.

For validation of the complete system, three test sessions were carried out. The first session collected the vibration data for validating the simulator model and the suitability of the data processing methods used. The second, collected the force-displacement data for the airspring modeling. The third test session involved the testing of the entire seat and simulator system.

Validation of the virtual model is based on comparison of the tested and simulated data. The results are presented for steady-state sinusoidal inputs in the range 1,5 and 8Hz and also random inputs of 0.5-20Hz. Analysis of the whole body vibration evaluation parameters like peaks, crest factor, rms, rmq (root-mean-quad), VDV (vibration dose value) and eVDV (estimated VDV) is also included.

The results obtained in this study indicate that the virtual model is able to reproduce the vibration behavior of the prototype fairly accurately in the 5Hz target region. With higher frequencies, the results shown that the model is not able to capture the nonlinearities observed in the prototype's response. The model, however, did exhibit its ability to predict the behavioral trends in the seat response which can prove to be very beneficial for seat design. Based on the level of agreement between the tested and simulated values for the whole body vibration parameters, the use of this model for whole body vibration evaluations looks promising.

Contents

List of Tables

List of Figures

Chapter 1

Introduction

A commercial vehicle driver's environment differs from that of a passenger car driver's, principally in two ways. One, drivers are exposed to road vibrations for prolonged periods of time, typically over 12 hours a day and second, the amplitude and frequency of the vibrations are in a greater and more importantly hazardous range for the human body. The branch of engineering dedicated to the study of effects of vibration on the human body is *whole body vibrations*.

1.1 Motivation

The nature and the associated effect of whole body vibrations vary by application.The application of interest here is the commercial vehicle cab and the type of vibration exposure is mainly vertical vibrations. The various studies in the field and the laboratory documented in the literature [4] indicate that the most common occupational injury associated with commercial vehicle drivers is lower back disorders. The upper lumbar and lower thoracic vertebrae have been noted to suffer the most damage [4]. The intervertebral discs mainly consist of Annulus Fibrosus and Nucleus Pulposus and these discs provide the flexibility to the spine. Studies by Frymore and Pope [3] suggest that bending and dynamic shear caused by the excitation of the bending mode of the lower spine cause a fatigue breakdown of the annular lamellea leading to degeneration of the nucleus pulposus. The experiments on human subjects to study this vibration disorder identify the frequency range of 4-8Hz as the cause of the first bending mode of the spine. The lumped parameter and finite element models [11, 12, 18] support these findings. The bending mode is characterized by translational and rotational motion between lower back vertebrae causing the above mentioned bending and dynamic shear at the intervertebral discs.

Due to these implications of vibration exposure in commercial vehicles the truck seat design assumes an increased importance and necessitates a critical review as it serves as the primary interface between the driver and the vibration environment. In recent years there has been a continued effort for regulating the vibration exposure for truck drivers through stricter norms on exposure limits and hours of service. It light of these newer guidelines and research in whole body vibrations a comprehensive seat design process is being researched by Commercial Vehicle Group (CVG) with Dr. Jack Wasserman guiding the research at the University of Tennessee, Knoxville. The design progresses ground up reaching the objective of developing a safer more comfortable seat design and improve market competitiveness. The main steps involved are listed below.

1. Data Acquisition: Collect vibration data on cab floor that would house the seat and also on the existing seat itself. This data collection is performed on roads that would be representative of the major transport routes of the region.

2. Data Analysis: Analyze the data based on methods relevant to whole body vibration evaluations. For example, rms (root mean square), peak factor, crest factor VDV (vibration dose value) and eVDV (estimated vibration dose value) etc. [4]. This provides the nature and characteristic of the vibration exposure of the particular region and make of the vehicle thus serving as design input to the seat development.

3. Optimization Using Virtual Model: A dynamic model of the seat in a virtual environment serves as an ideal parameter optimization stage in the design process. Here the floor vibration data serves as the input and the relevant vibration parameters at the points of interest on the seat will be the output. These can be checked against the vibration standard for compliance and also to quantify the performance improvement over the existing seat. The virtual model lends itself to seat performance optimization for the truck and roads characteristic to a region or country by allowing fast design of experiments (DOE) saving the time required for physical setup. The virtual model will also help evaluate the performance of the seat against the whole body vibration standards like ISO 2631, BS 6841, ANSI S3.18, etc.

A crucial step in this process is the development of the virtual dynamic model of the seat and this forms the basis of this research. The aim is to develop a dynamic model of the seat and to verify its feasibility and accuracy for reproducing vibration behavior, enabling it to take its place in seat design process.

1.2 Objective

The main objectives of this thesis are to-

1. Develop a multibody dynamic model of a truck seat and the 6 axis MTS simulation table using the commercially available multibody dynamics code MSC.ADAMS.

2. Identify appropriate data processing methods for using the measured vibration data as input to the dynamic model and evaluate the accuracy of the process.

3. Evaluate the accuracy of reproduction of models vibration behavior by comparing the output with that measured from prototype tested on the MTS 6 axis simulation table.

The MTS simulation table model was previously developed by National Seating, but was not verified against vibration data collected. The accuracy of the simulator model's dynamic response is directly responsible for the accuracy of the seat's dynamic behavior as it is in the physical test loop at National Seating's testing lab at Vonore, TN.

Thus the objective of this research was to develop a dynamic model of a truck seat system along with the MTS 6-axis simulator, to determine its accuracy and therefore the feasibility within the envisioned design process. This accuracy and feasibility testing is specifically targeted for the frequency requirements of whole body vibration evaluations.

1.3 Scope of Thesis

This thesis covers the development of a multibody dynamic model of a suspension truck seat. The process involves importing the CAD model for the complete seat model into the multibody dynamic software. Using idealized joints and forces the discrete CAD model is transformed into a rigid multibody dynamics model. In order to validate the model's response to vibration input a prototype seat was tested at National Seating's test facility. The data collected at the test was then used as reference data for the simulated response. The model's response was evaluated using time and frequency domain analysis along with parameters relevant to whole body vibrations.

The CAD model was previously developed by National Seating in UniGraphics and was available in a parasoild format. This was then imported into the multibody dynamics software MSC. ADAMS/VIEW. In ADAMS the various joints, forces and input motions were incorporated making the model ready for simulations. The pre-simulation data processing as well as the post-simulation data analysis was performed using Matlab/Simulink.

The scope of this thesis is limited to the development and validation of the rigid multibody dynamic model of the truck seat based on laboratory tested sine and random input

in the vertical direction only. The verification of the model's response in the horizontal directions is not covered in this thesis.

1.4 Organization of Thesis

This thesis is organized into eight chapters. Chapter 2 provides a basic background of truck seats, their necessity and data acquisition methods typically used in vibration data collection. Chapter 3 details the data processing methods used to transform the raw acceleration data into a form usable by the dynamics code. It covers the filtering and the numerical integration processes employed in the pre-simulation data processing phase. Chapter 4 describes the test setup, the requirements and goals of each test session. It also gives an account of the various input signals used for testing the prototype. Chapter 5 gives a detailed description of the development of multibody dynamic model in MSC. ADAMS/VIEW. It provides the implementation methods used to model the main components of the seat - the suspension mechanism, airspring, dampers and the seat cushion. Chapter 6 includes the time and frequency domain plots for comparing the tested and simulated responses. The results are provided for plots for sinusoidal (1Hz, 5Hz and 8Hz) and random (0.5-8Hz) inputs. Finally, from the results in Chapter 6, the derived conclusions, the limitations of the modeling process and the direction for future research are discussed in Chapter 7.

Chapter 2

Background

2.1 Need of Suspension Seats in Trucks

The primary difference in a commercial vehicle and a car starts with its purpose. While a car is only used for passenger transport, the commercial vehicle is used for transport of goods and heavy equipment across longer distances. The chassis suspension design not only has to satisfy the comfort requirements but also stable and safe vehicle dynamics requirements. A general rule of thumb in suspension design is that softer suspension promotes comfort, while stiff suspension promotes improved vehicle dynamics. For the passenger car with its low center of gravity and low sprung mass, reaching a balance between comfort and safe vehicle dynamics is relatively easy. However, for a commercial vehicle the comfort requirements take second priority over safe vehicle dynamics and maximum payload capacity. Due to the much higher payload capacity and high center of gravity the chassis suspension in a truck is much stiffer. This results not only in higher magnitude of the acceleration transmissibility to the cab and the driver, but also higher first resonance frequency. A typical passenger car has its first resonant frequency in the range of 0.9-1.5Hz (well below the 4-8Hz range), while for a commercial vehicle typical values are 2-3Hz (much closer to the 4-8Hz range). Figure. 2.1 illustrates a simple two degree of freedom quarter car model for a truck and a car. The typical values for the suspension parameters are given in Table. 2.1 [10, 14]. The transfer function for the 2-dof system shown Figure. 2.1 is given by

$$\frac{X_s(s)}{X_r(s)} = \frac{b_s b_t s^2 + (b_t k_s + b_s k_t)s + k_t k_s}{m_u m_s s^4 + (m_u b_s + m_s b_t)s^3 + (m_u k_s + m_s k_t + b_s b_t)s^2 (b_t k_s + b_s k_t)s + k_s k_t} \quad (2.1)$$

The $X_s(s)$ and $X_r(s)$ in (2.1) represents the the sprung mass and road input displacement in the Laplace domain. Figure. 2.2 shows the frequency response for the transfer function.

Table 2.1: Typical suspension parameters for a truck and car

Parameter	**Truck**	**Car**
Sprung mass (m_s) kg	4450	730
Unsprung mass (m_u) kg	1000	63
Suspension Stiffness (k_s) kN/m	1000	36.3
Tire Stiffness (k_t) kN/m	1500	182.47
Suspension Damping (c_s) kNs/m	25	3.92
Tire Damping (c_t) kNs/m	4	0.1

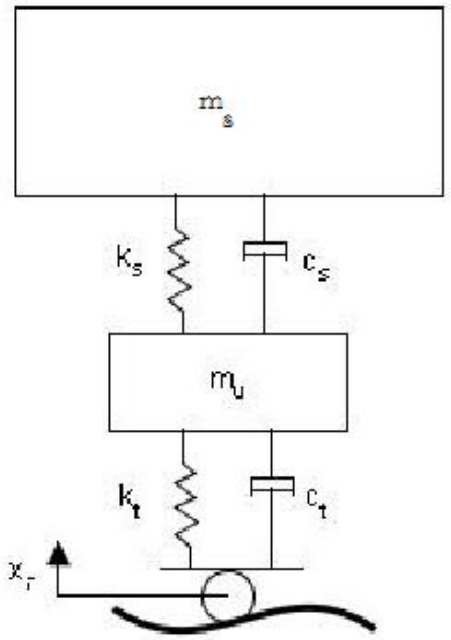

Figure 2.1: Simple representation of two degree of freedom suspension system

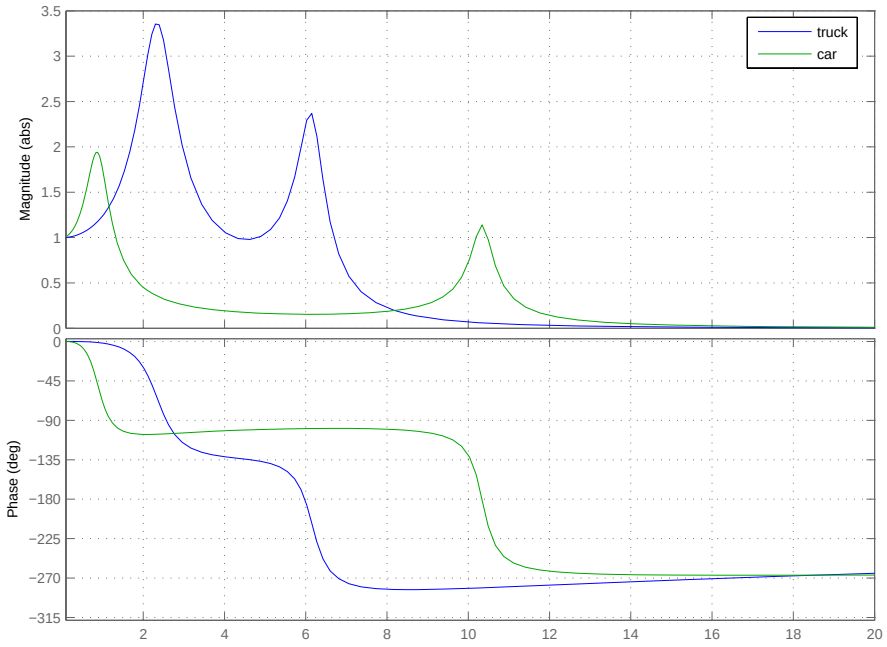

Figure 2.2: Comparison of frequency response (bode plots) for truck and car suspension system

This is a simplified representation of the suspension systems, however it effectively demonstrates the need for additional vibration and shock isolation system for the trucks. This is the main reason why trucks have suspension seats and cars do not.

The truck seat suspension traditionally used metal springs for shock and vibration isolation. The deflection of the isolator under dead weight is inversely proportional to the square of the natural frequency. So for a linear spring, the lower the natural frequency, the higher is the static deflection. This results in a situation where acceptable frequency response produces unacceptable displacement amplitudes for the drivers. Another point of consideration is that for a metal spring, as the driver weight changes the static equilibrium height changes and therefore the effective stroke limits are altered. Most contemporary seats now have *airsprings* in place of metal springs. An airspring unlike metal springs, uses a gas, mostly air, as its potential energy storage element [6]. Due to the compressibility of the gas the energy stored per unit volume for an airspring is high and so it does not require high deflection to produce low natural frequency. The gas can be compressed to support the load without affecting the stiffness or the compressibility of the gas. Also a driver of any weight can be supported on the seat at the same design static equilibrium height by simply changing the initial pressure. The main components of the seat that affect the vibration isolation characteristics are

1. Energy Storage Element- Air Spring
2. Damping Element-Viscous Damper
3. Secondary Isolation Element- Seat Cushion
4. The Linkage Mechanism- Scissor or the X-Arm Mechanism

The accuracy of modeling these elements will directly affect the accuracy of the dynamic response of the virtual model.

2.2 Data Acquisition

In order to study the nature of the vibrations experienced by the driver we need to quantify the vibration signals. Choices available for measuring the motion are displacement, velocity and acceleration.

Selection of Measured Parameter: Displacement and acceleration measurements prove easier quantities to measure compared to velocity. So if velocity is a required quantity,

it is almost always derived from displacement by differentiation or integration of acceleration. In fact from (2.2) any convenient quantity can be measured and the rest can be derived by either integrating or differentiating the measured quantity [1].

$$a = \frac{d^2 s}{dt^2} \qquad\qquad v = \frac{ds}{dt} \tag{2.2}$$

The differentiation process inherently amplifies noise while integration reduces noise and therefore integration can be effectively used to determine velocity and displacement from acceleration. Also acceleration is directly related to the inertial force through Newton's second law, thus proving as the ideal quantity to be measured for vibration studies. Almost all the vibration standards specify the limits and evaluation methods in terms of acceleration levels. There are two types of commonly used accelerometers

- Capacitive
- Piezoelectric

For acceleration measurements in the frequency range of 0.5-20Hz the capacitive type triaxials and uniaxials have been used in this study. The accelerometers measure the acceleration in units 'g', the acceleration due to gravity.

Accelerometer Positioning: To study the vibration input to the seat base the cab floor needs to be instrumented with accelerometers at least at three locations. Three pickups are required as three (noncollinear) points completely define the position and orientation of a plane is space. For the best accuracy the three points should be as far from each other as possible. However, this makes measuring the accurate relative positioning difficult. Another important point here is that the position of at least one of the accelerometers should be accurately known from a landmark on the seat. This establishes the position of the seat on the moving plane. The following scheme will provide a comprehensive representation of the vibration input to the seat and seat's dynamic behavior

- Three accelerometers on the cab floor
- Three accelerometers on the seat frame above the isolation element but below the seat cushion
- Seatpad accelerometer at the interface of the driver and seat cushion
- Seatpad accelerometer at the interface between driver's back and seat back cushion

The accelerometers on the cab floor define floor motion and therefore vibration input to the seat. The accelerometers on the seat frame define the motion and orientation of the seat frame. With proper vector calculations this will provide information not only about the vertical compliance but also the lateral and longitudinal bending of of the suspension mechanism. This part is not addressed in this research as the model built is a rigid model. Future work on the model would include making the critical suspension mechanism component as flexible bodies, giving the model increased accuracy. For information of the transducer positioning for the laboratory tests please refer sec. 4.3

Chapter 3

Data Processing

As mentioned in section. 2.2, the accelerometers record the acceleration in units 'g' i.e. acceleration due to gravity which, in SI system is $9.81 m/s^2$. The format of the stored data varies with the data acquisition system used. The system used during the tests recorded the data in a .RPC format. This data was then converted into .mat (Matlab's data format) files, using a data analysis software called FlexPro 7.0. Some systems like the Dewetron Data Acquisition can record the data in a .mat format, saving this step in processing the data. Matlab serves as an excellent tool for data analysis and signal processing with a comprehensive library of functions for filtering, numerical integration and fast matrix computations. The sections 3.1 to 3.4 explain the steps involved in preparing the data acquired in the field, for use by ADAMS to run simulations. Figure 3.1 gives an overview of the data flow from acquisition to analysis.

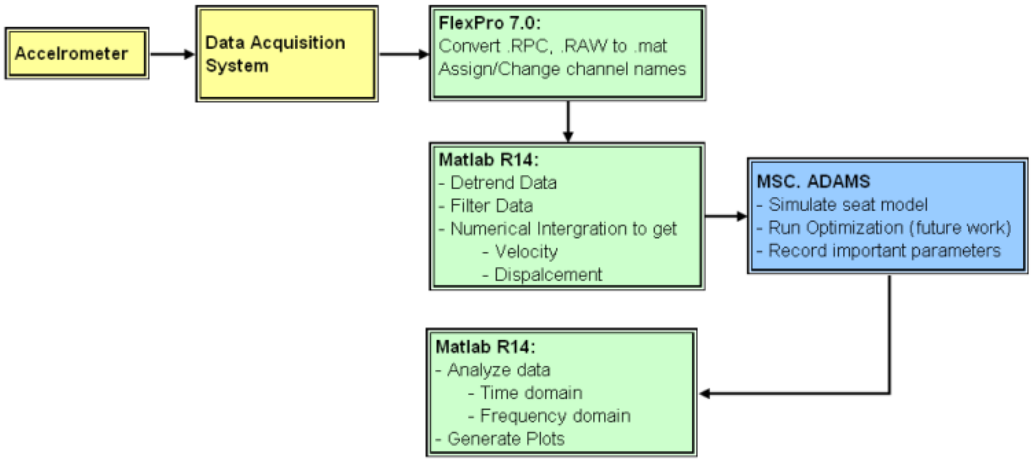

Figure 3.1: An overview of the flow of data from acquisition to analysis

3.1 Data Segmentation

The collected data can be a time series of large durations, as long as 2-4 hours. With a typical sampling frequency of 512Hz and an average of 24 (8 triaxial accelerometers) channels of data, such a duration will represent a data matrix of size $3.68E^6$ x 24. The whole body vibration standards and most of the literature in this field report the evaluation measures over time durations not exceeding 240 sec. So the data needs to be segmented to the required length (eg. 8, 16, 30, 60, 120, 240 sec)and only the segments of interest can be selected for further processing saving considerable amount of computational resources.

3.2 Data Filtering

The raw data collected almost always contains noise and a DC error introduced in the measured signal. The input to the dynamics code can be either displacement, velocity or acceleration. Each of these is handled differently by the ADAMS/Solver to calculate the states of the dynamic system during simulations.

- Displacement: To use displacement as an input, the measured acceleration needs to be doubly integrated during the data processing phase. Any drift or noise in the signal will continuously accumulate with increasing time during the integration process.
- Velocity: To use velocity as an input, the measured acceleration needs to be integrated once. However the dynamics code will integrate the signal once for displacement within its own solver and will suffer from similar integration errors.
- Acceleration: In this case no integration is required at the data processing stage but the ADAMS/Solver will perform the double integration leading to the same consequences.

Fig. 3.2 illustrate these problems

To address this issue the data is first detrended. This removes any linear trend in the data thus centering the data about zero. The second step is to bandpass the data through a filter. The frequency range of interest in this application is 0.5 to 20Hz so these limits serve as as corner frequencies for the Butterworth bandpass filter used. The same data used to illustrate Fig. 3.2 is first filtered and then integrated. Now the result is sensible velocity and displacement values. This is shown in Fig. 3.3. More advanced techniques in signal processing are presented in [13, 21].

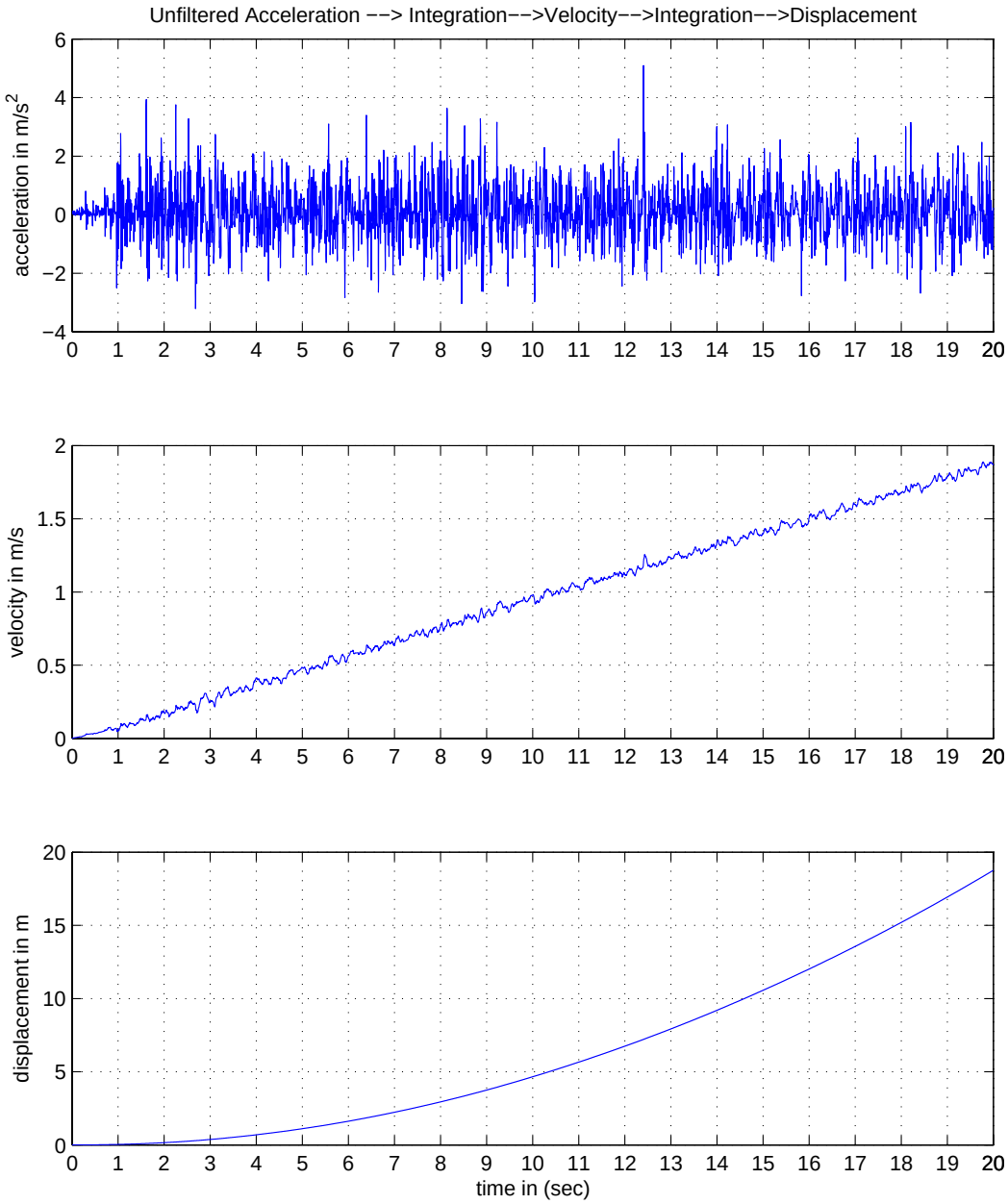

Figure 3.2: Example of accumulating error with time in the integrated velocity and displacement from unfiltered acceleration signal

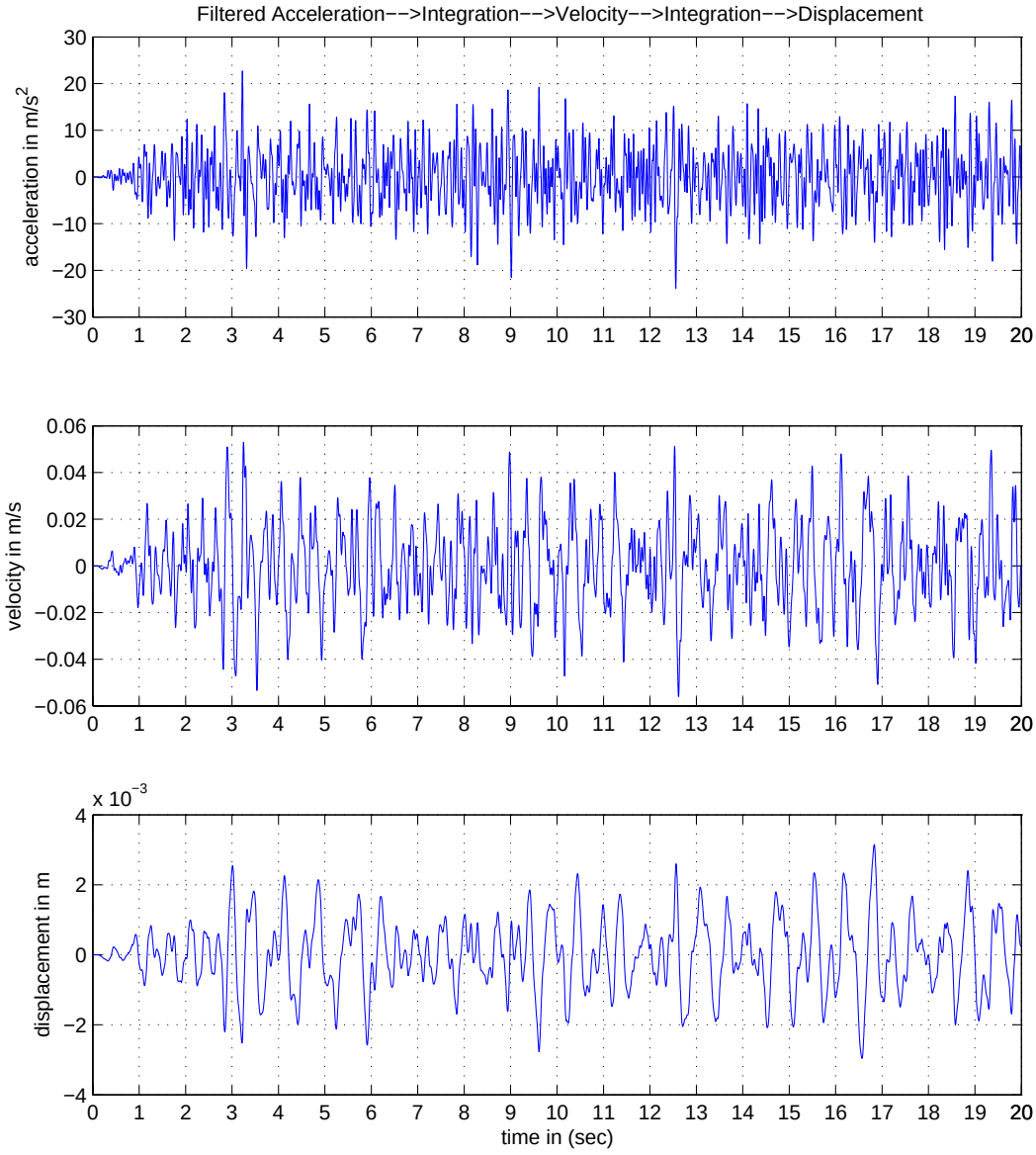

Figure 3.3: Example showing correct computation of the integrated velocity and displacement from detrended and filtered acceleration signal

3.3 Data Integration

Once the measured acceleration data is detrended and filtered it can be integrated to produce velocity and displacement using any suitable numerical integration methods. Here the acceleration has been integrated using 4th order Runge Kutta (ode45) routine implemented in Simulink. Simple trapezoidal rule integration would be sufficient if the integration steps taken by the dynamics code solver were larger than that used for integration.

3.4 Matlab GUI Development

Each data collection exercise can differ in number of channels collected, channel names, length of data, sampling frequency etc. So these data processing Matlab codes need to be modified each time with respect to number of channels, names, segment location and length etc. So to increase the flexibility and userfriendlyness a Matlab GUI was developed. This GUI streamlines the whole simulation process from data processing to plotting the results. Some useful functions of the GUI are listed below.

- Load all channels and allow selection of channels for data processing. Figure 3.4a
- View the acceleration for the selected channels in time domain and provide data segmentation options. Figure 3.4b
- Filter the data and provide options to choose corner frequency for the filter. This section also provides a frequency domain representation of the data to help identify the nature of the frequency content. Figure 3.4c
- Allow the allocation of channels to corresponding inputs to the dynamics code. Matlab can directly communicate with MSC ADAMS to supply the input signals. Figure 3.4d.
- Control the dynamic simulation from within Matlab and accept the simulation result sets for further analysis and comparison with the measured data.

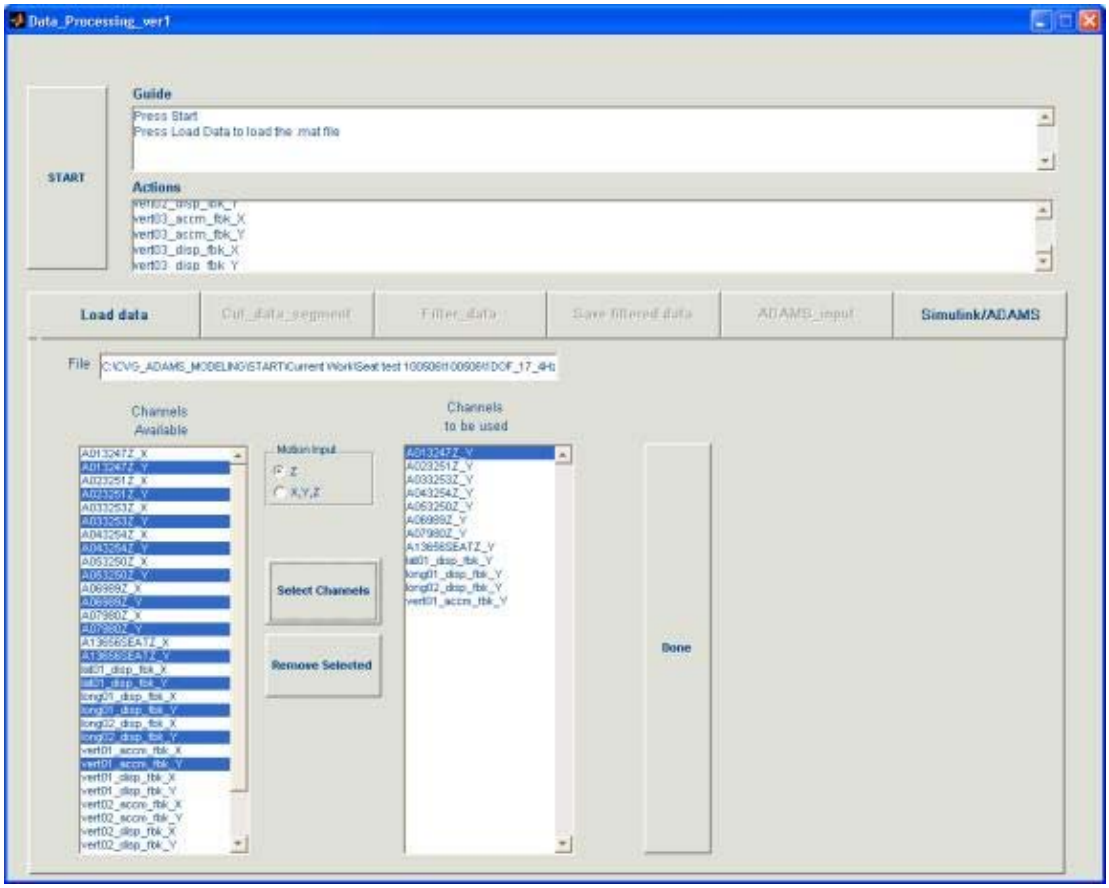

Figure 3.4a: Tab- Load data file and select channels.

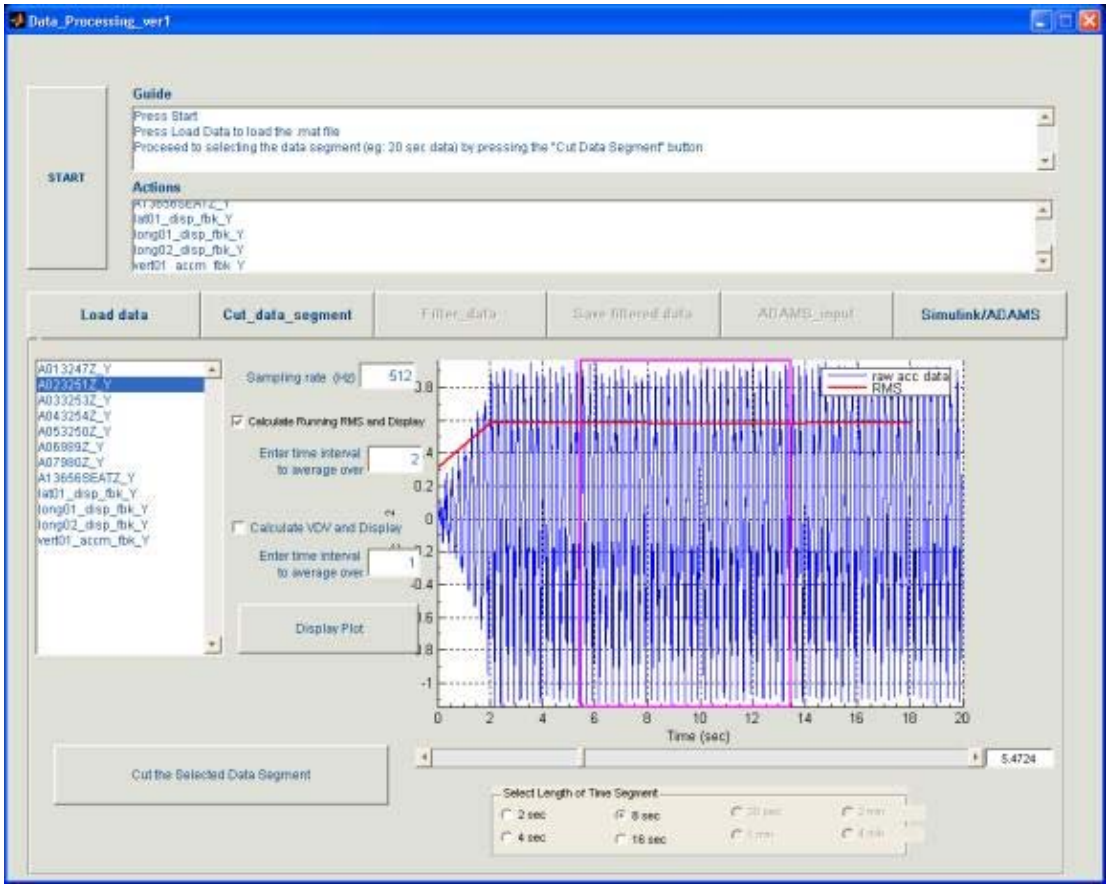

Figure 3.4b: Tab- Review channels and select segment of interest

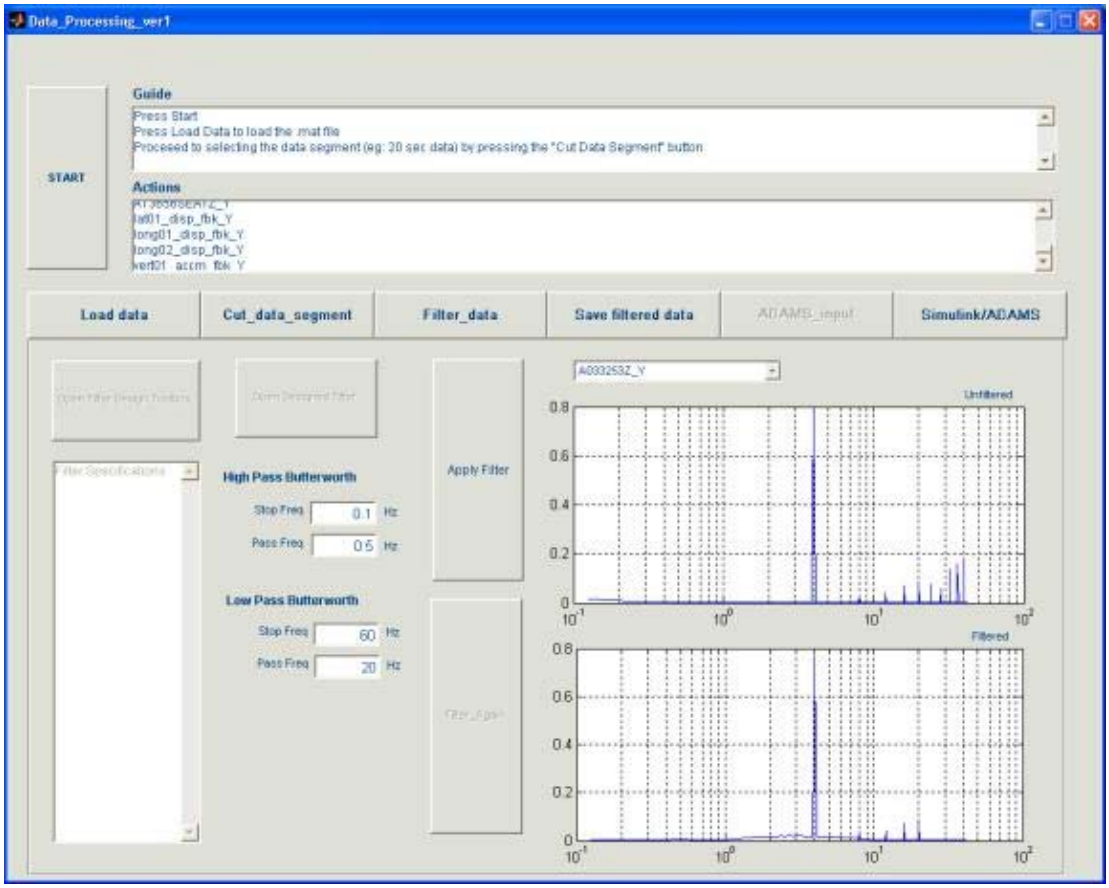

Figure 3.4c: Tab- Filter data and compare filtered and unfiltered data.

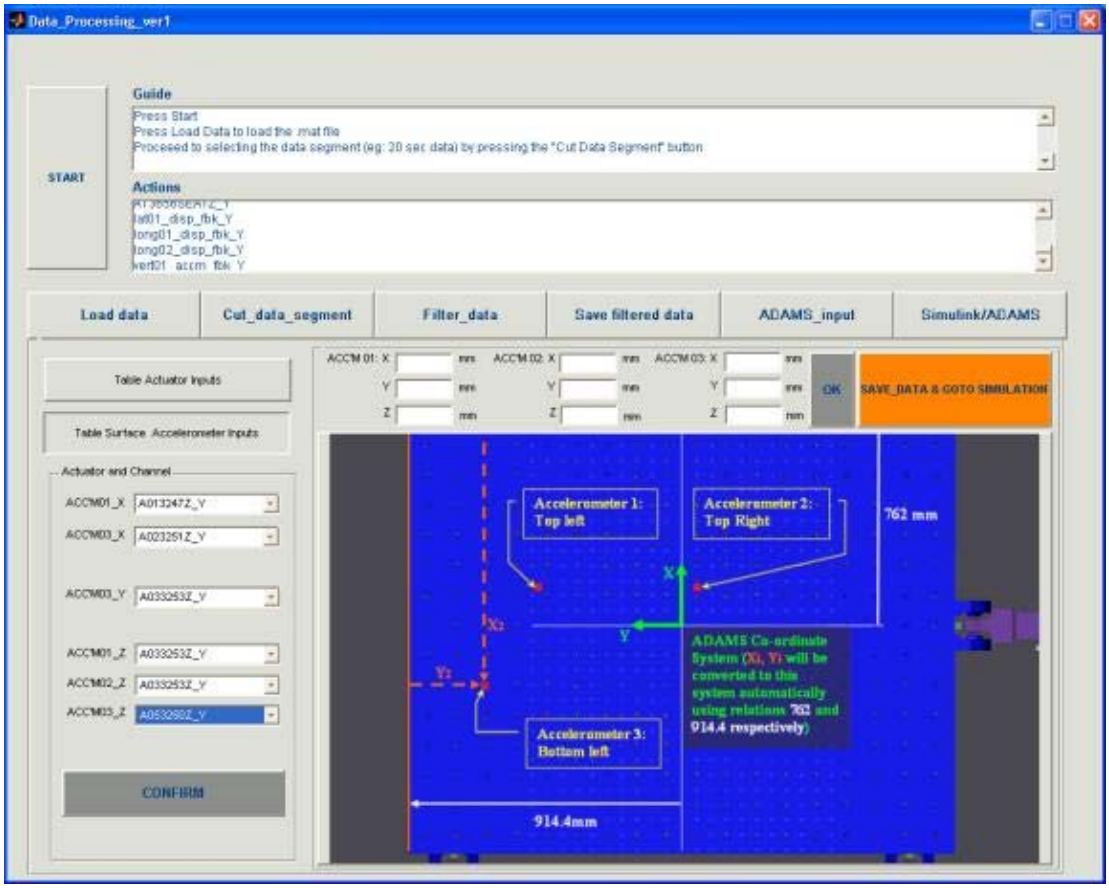

Figure 3.4d: Tab- Associate channels to appropriate Adams inputs.

Chapter 4

Testing and Experimental Setup

For a mathematical model to qualify for any practical use, the most important step is the validation of the model. To verify the vibration behavior of the seat model, a prototype was tested at National Seating's testing facility at Vonore, TN. The prototype was tested on the MTS Multi-axis Vibration Simulator. The vibration simulator generates the real world vibration environment in a laboratory setting. This simulator is used by National Seating for their design development as well as durability testing. Since this simulator plays a key role in testing, it was also included in the modeling process. This entails testing the simulator model first to ensure that the vibration input to the prototype and the virtual model are identical. The overall testing was divided into three parts each with a specific objective

1. Test session 1- The MTS simulator was tested as a separate system. This test was used to collect the data intended for the verification of the simulator model.

2. Test session 2- The seat was fixed to simulator table and the session was used to collect data for deriving the air spring force as a function of spring length.

3. Test session 3- With the seat fixed to the simulator table, this test was used to collect data for verifying the complete system response.

4.1 Setup for MTS 6-Axis Simulator Testing

Here the MTS simulator was tested as a separate system, so that any deviation of the simulator model form the measured data can be identified and taken into consideration when comparing the seat model behavior as it is the primary aim of this study.

Table 4.1: Inputs for MTS simulator testing

	Input Type	**Amplitude(m)**	**Frequency(Hz)**	**Axes**
1	Sinusoidal	0.02	0.5	XYZ
2	Sinusoidal	0.02	4.0	Z
3	Random	0.00635 (rms)	0.5-20	XYZ

Setup and Instrumentation The surface of the simulator table was kept empty and was instrumented with four accelerometers. As mentioned in section 2.2 only three accelerometers are sufficient. The relative distances between the accelerometers as well as the position of one with respect to the table reference were noted. These were correspondingly used to place the accelerometer markers in the ADAMS model. Figure 4.1 shows the placement of accelerometers used for the test.

The system was tested for sinusoidal and random inputs. The inputs were displacement signals provided to the six actuators driving the simulator, while the surface accelerometers, feedback accelerometers and the feedback LVDTs were the measured signals. Table 4.1 provides details about the input signals.

Data Collections Out of the four accelerometers only the three having the maximum separation were selected. Each accelerometer has three channels of data corresponding to the X,Y and Z directions. This makes a total of nine channels (space variables) to define the 6-dof motion of the table surface. So out of nine only six were selected, three-Z, two-X and one-Y. The MTS simulator has its own feedback accelerometers and LVDTs at its six actuators. The signals from these built-in transducers were also collected. The simulators data acquisition system accepts all the transducer inputs including the external accelerometers in a single system. This ensures all have precisely the same sampling instance. The data is then processed as explained in Chapter 3. This processed data is then used as an input to the ADAMS simulator model. The section 6.1 discusses the comparison of the simulated and tested values.

4.2 Setup for Airspring Data Collection

The airspring used as the isolation element in the prototype was also a development prototype from Firestone and so the airspring force-displacement curve was not available for use in the dynamic model. This test session was conducted in order to obtain the force-displacement characteristics of the airspring. Another important reason for this test, even if the spring manufacturer's data were available, was that the manufacturer's data gives

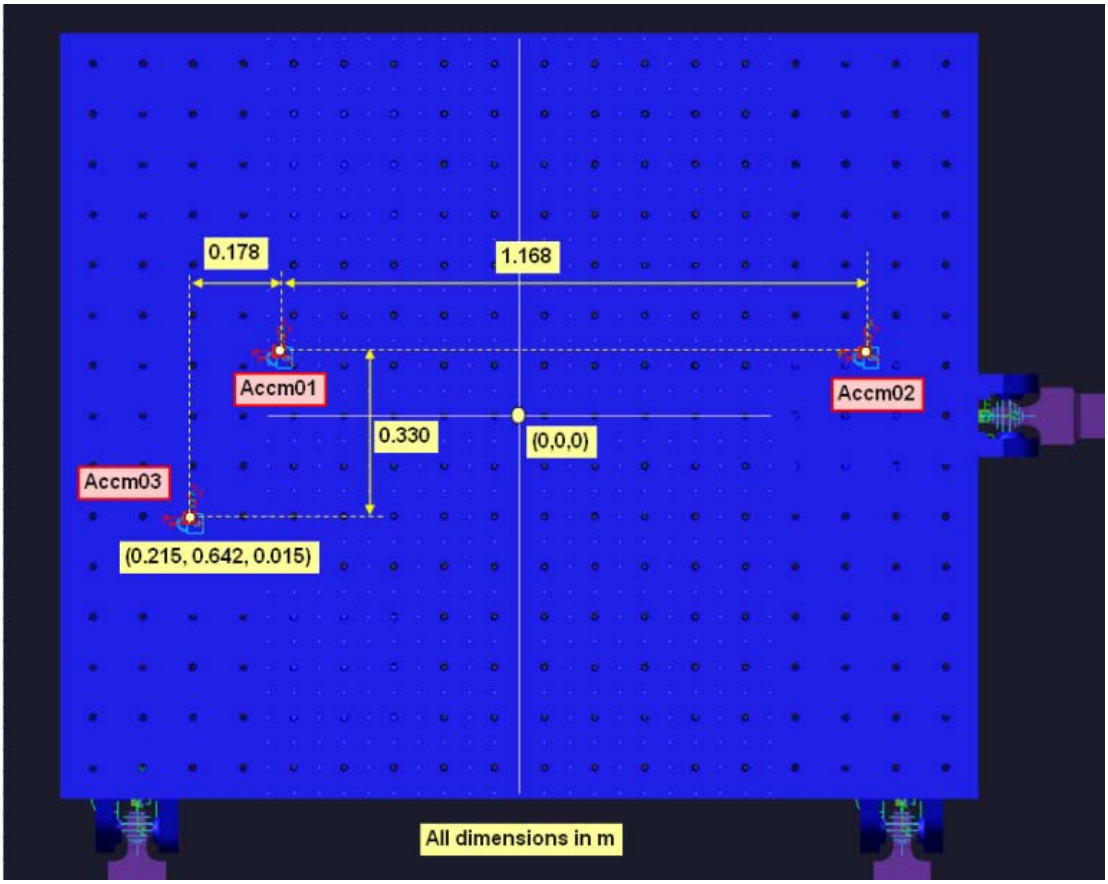

Figure 4.1: Accelerometer placement for simulator testing setup

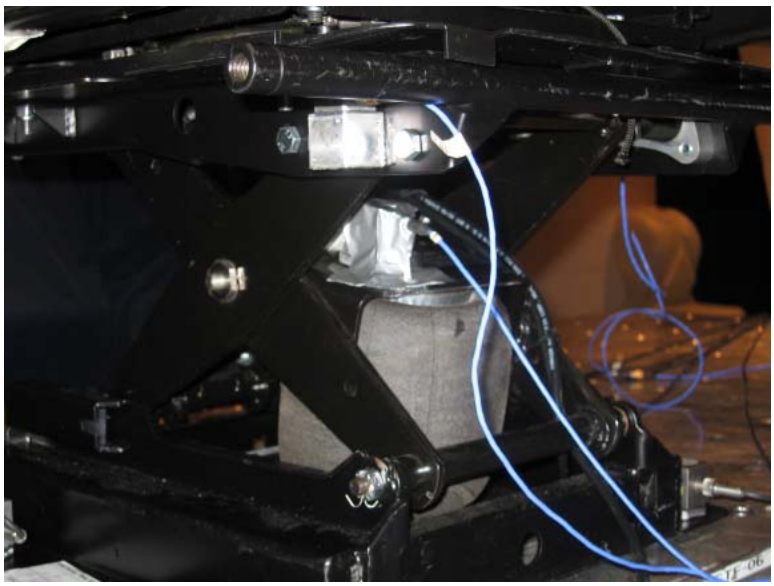

Figure 4.2: Airspring instrumented for force data measurement

force generated with a pure axial compression. In this suspension design, fixed plates (non-pivoting) attached to the moving X-arms control the compression of the spring. This results in the springs lateral stiffness also contributing to the force between the two points of application. So the need to obtain the spring force as a function of spring length in the installed configuration justified this test session.

Setup and Instrumentation For this test a washer type force load cell was added in series with the airspring and the load cell data was recorded as the measured quantity. One accelerometer was fixed to the base of the seat frame and another uniaxial was fixed to the top plate of the airspring. A sinusoidal input at 1 Hz and an amplitude that produced at least 75% of the allowable travel on the mechanism, was used as input. This resulted in a signal with frequency 1Hz and an aplitude of $0.02m$. The setup is as shown in Fig. 4.2

Data Collection The force load cell records the force developed by the airspring as a function of time during the test run. As seen in Fig. 4.2 there was no place to install an LVDT to measure the airspring length as a function of time, thus requiring a unique approach. The table motion and so the spring's base motion in space was known from the base accelerometer and that for the spring top from the accelerometer fixed to the spring top plate. Now, the motion of both the base and top of the spring are available with respect to the same inertial reference (earth). Thus, doubly integrating the acceleration of both accelerometers as explained in Chapter 3 gives the displacement signals which were used to

drive the point motion at the corresponding top and bottom spring points in the virtual model. Now, a measure function can be easily programed in the ADAMS model to compute the length between the two spring end points. This gives the spring length as a function of time. Now we have both force as $f(time)$ and spring length as a $f(time)$ and the time for both is the same as they have been recorded simultaneously. Therefore we can finally get the force as a $f(length_{spring})$. Figure 4.3 shows the plots for force, spring length as a $f(time)$ and then the force as a $f(length_{spring})$.

4.3 Setup for Seat-Simulator System Data Collection

This was the main test session where the complete seat and simulator system was tested. The data collected during this session was used to eventually validate the accuracy the systems dynamic behavior. The prototype seat used in the test is shown in Fig. 4.4

Setup and Instrumentation For this test the seat was bolted to the simulator table surface. Three accelerometers were fixed to the base of the seat frame. These would provide the necessary data to define the base vibration input to the seat. The next set of three accelerometers was fixed to the seat frame above the isolator and damping element. These accelerometers provided the vibration information after passing through the primary seat suspension. Figure 4.5a to figure 4.5c show the accelerometer positions. To measure the vibration at the seat cushion and dummy weight interface a seatpad was taped to the surface of the seat cushion. The seatpad provided the vibration input to the dummy weight and so the driver in an actually truck cab. All the accelerometers were connected to the simulator's data acquisition system so the data could be collected in sync with the driving motion data. Fig. 4.6 shows the complete setup for this test. The tests were again run for sinusoidal and random inputs, the details of which are provided in Table. 4.2

Data Collection and Processing For this test a total of 20 channels of acceleration data and six channels of displacement data (actuator displacement feedback) was available. The data channels selected for processing and input to the dynamic model are given in Table. 4.3. This data is then processed for input to the virtual model in MSC. ADAMS/VIEW.

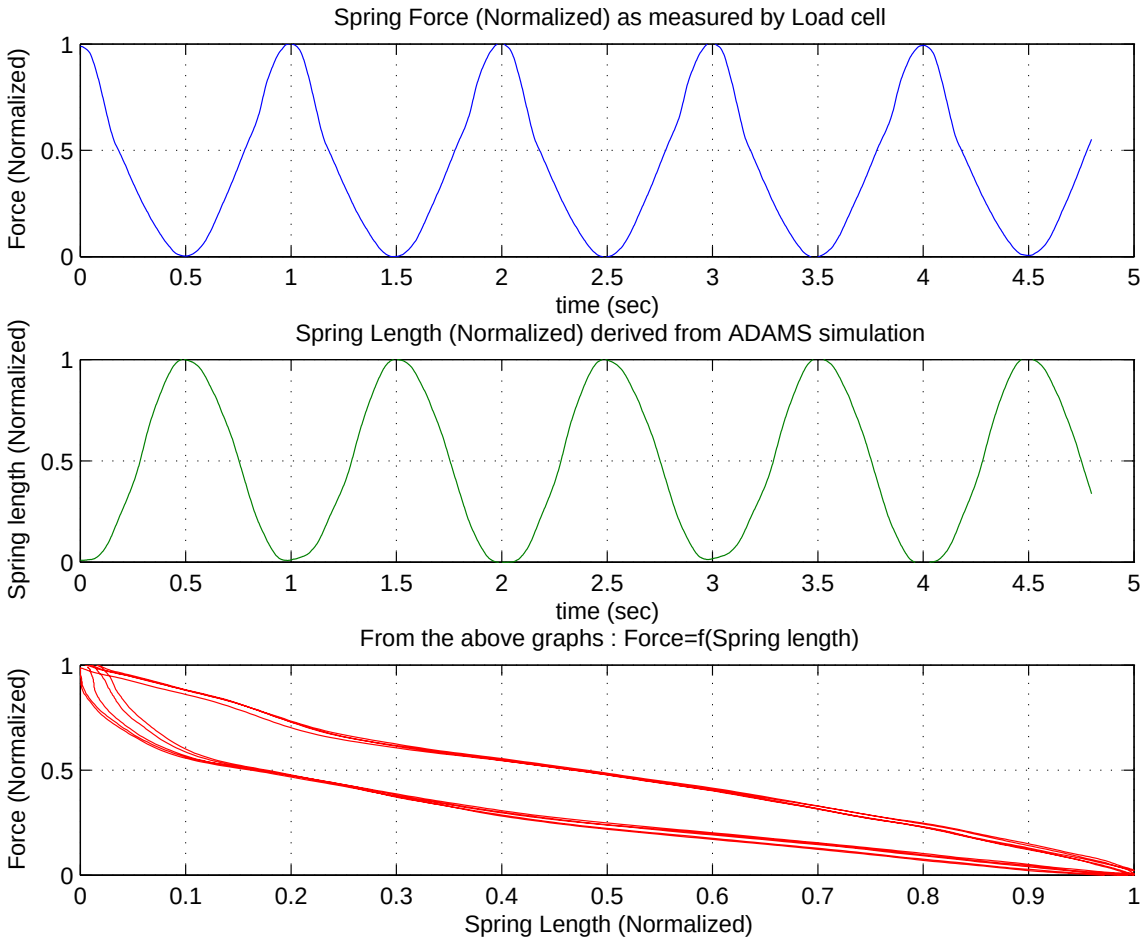

Figure 4.3: Airspring test: Force,spring length as a function of time leading to force as a function of spring length

Figure 4.4: Seat Test: Prototype seat used for testing

Figure 4.5a: Seat test stepup:Accelerometer instrumentation front view

Figure 4.5b: Seat test stepup:Accelerometer instrumentation left view

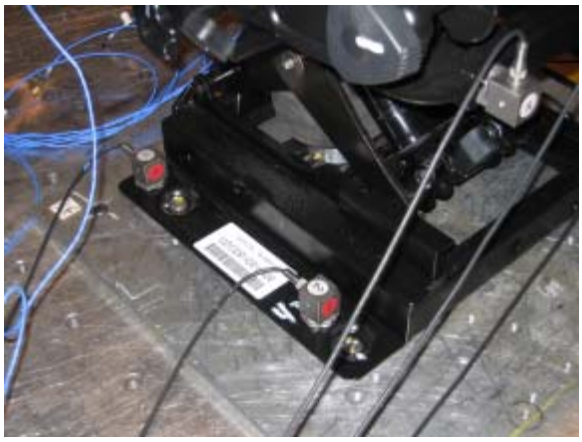

Figure 4.5c: Seat test stepup:Accelerometer instrumentation right view

Figure 4.6: Complete seat test setup

Table 4.2: Inputs for seat-simulator combined system testing

	Input Type	**Amplitude(m)**	**Frequency(Hz)**	**Axes**
1	Sinusoidal	0.0127	0.5	Z
2	Sinusoidal	0.0127	1.0	Z
3	Sinusoidal	0.0127	2.0	Z
4	Sinusoidal	0.0127	3.0	Z
5	Sinusoidal	0.0127	4.0	Z
6	Sinusoidal	0.0127	5.0	Z
7	Sinusoidal	0.0127	6.0	Z
8	Sinusoidal	0.0127	7.0	Z
9	Sinusoidal	0.0127	8.0	Z
10	Chirp	0.0127	0.4-7	Z
11	Sinusoidal	0.0254	0.5	XYZ
12	Sinusoidal	0.006	4	XYZ
13	Random	0.0365(rms)	0.5-20	XYZ
14	Random	0.0365(rms)	0.5-20	XYZ

Table 4.3: Data channels selection for seat-simulator test

Accm No.(test)	**Accm No.(Model)**	**Channels**
1	3	X,Z
2	2	Z
3	1	X,Y,Z
4	4	X,Y,Z
5	5	X,Z
6	6	Z
7	7	Z
Seatpad	Seatpad	X,Z

Chapter 5

Model Development

This chapter gives an account of the modeling of elements that play a major role in defining the dynamic behavior of seat system. These elements are the

- Suspension mechanism
- Airspring
- Viscous Damper
- Seat Cushion

Sections 5.1 to 5.4 elaborate on modeling of these elements.

5.1 Model Construction

In order to get the dynamic behavior of the model close to that of the prototype, the suspension mechanism needs to be dimensionally accurate. This will result in an accurate kinematic behavior assuming a rigid nature of the metal components. The most convenient way to do this is by importing the CAD model for the tested prototype. The CAD model was available in UniGraphic's parasolid format from National Seating. ADAMS also has parasolid as its basic CAD format and so the CAD exchange was seamless. Figure 5.1 shows the CAD model and prototype photos side by side.

Not considering the manufacturing errors in the production of the prototype, the CAD model represents an accurate geometry of the seat prototype. The CAD model exchange also ensures the mass and inertia properties of all the components, except the foam parts, to be accurate within practical limits. Since this model has a potential for use in optimization of the various parameters like mechanical advantage, spring and damper motion ratios and force characteristics, some level of flexibility for modification of these needs to be

Figure 5.1: CAD model imported into ADAMS and Prototype photo

built into the ADAMS model. To achieve this goal, prior to importing the CAD data into ADAMS, a skeleton of ground points was created to represent the hardpoints of the suspension mechanism, spring, damper and cushion. For this the point location information was extracted from the CAD data within ADAMS, but in a different modeling file. These points were then connected with massless entities like lines and planes. All the force elements and joints were defined at this stage of modeling. However, no dynamic simulation can run at this stage as there are no inertia elements defined in the model yet. Once all the joints and forces were defined, the CAD geometries were imported to merge with corresponding massless entities. So if the suspension configuration changes or the CAD model changes, only the inertia element can be replaced without disturbing the joints and the force. The suspension hardpoints including those for the spring and damper locations are parametrized, so they can be they can be modified easily during the optimization routines for future developments.

One important mass element in the model is the dummy weight. The dummy weight is used, as the prototype cannot be tested with a human subject. The MTS simulator is not certified for any live subject testing due to its very high acceleration capabilities. The weight used in the test was a 168lb (approx. 75kg) plastic can filled with sand.

5.2 The Airspring

The airspring is the main vibration and shock isolation element in the suspension system. The accuracy of the frequency response of the seat is dependent to a large extent on the accuracy of the force-displacement characteristic of this element. As mentioned in section 4.2 to obtain this force characteristic, the force was directly measured with a load cell, while the corresponding compression was derived from acceleration signals at the two ends of the spring. The details of the procedure used to arrive at the spring curve from the data collected are as follows

1. The force data was first filtered to remove the high frequency noise, while the acceleration was processed to obtain displacement as a function of time.

2. The force was then expressed as a function of displacement (section 4.2). The data was smoothed using Matlab's smoothing spline algorithm.

3. From Figure 5.2 it can be seen that there was a considerable amount of internal damping present in the airspring. To use the spring force curve in ADAMS, the compression and extension data were averaged so that a unique force value exists for each displacement value. Curve fitting was performed using this averaged force curve as reference. Using the curved fitted data in ADAMS enabled it to extrapolate the force value

correctly if the displacement in the model went beyond the displacement values available in the measured data. Figure 5.2 shows the plot of force against displacement as measured (and in part derived), the averaged compression and extension curve and the fitted (and extrapolated) data. To get the most accurate representation, the compression and extension parts were averaged correspondingly over several cycles.

ADAMS Implementation of the Airspring: The airspring was implemented in ADAMS using the SFORCE (Single Force) element. The SFORCE element generates a force between the two points (spring top point and spring bottom point)used to define the spring, along the line of sight. A cubic spline function was used to describe the SFORCE element. The force-spring length data is imported first imported into ADAMS. ADAMS then creates a spline element to model the force as a function of spring length by using a piecewise cubic polynomial. This enables it to perform the cubic interpolation during the simulations.

In order to account for the internal damping, a viscous damping element is added in parallel to the spring. This damping is modeled to generate a value of as $10 - 12\%$ of the force generated by the airspring. Figure 5.3 shows the airspring modeled in ADAMS.

5.3 The Viscous Damper

The dampers are installed in the suspension mechanism as shown in the Figure 5.5. The force-velocity curves for the viscous damper were available from the testing department at National Seating. Figure 5.4 shows a plot of normalized force-velocity relationship used to model the damping elements.

ADAMS Implementation of Damper Element: The damping elements are modeled as two SFORCE elements between the points on the suspension mechanism as shown in Figure 5.6. Similar to the airspring the force-velocity curve, as obtained from the test data sheet, was imported into ADAMS. ADAMS then fits a piecewise cubic polynomial to the data and uses the cubic spline function to interpolate force values during simulations.

5.4 The Seat Cushion

The modeling of the seat cushion is not as straightforward as that for the airspring or damper as the cushion's stiffness and damping are inherent material properties of the foam. The stiffness and damping properties of the foam are highly frequency dependent. Usable form of this data for dynamic modeling was not readily available and so it had to be estimated

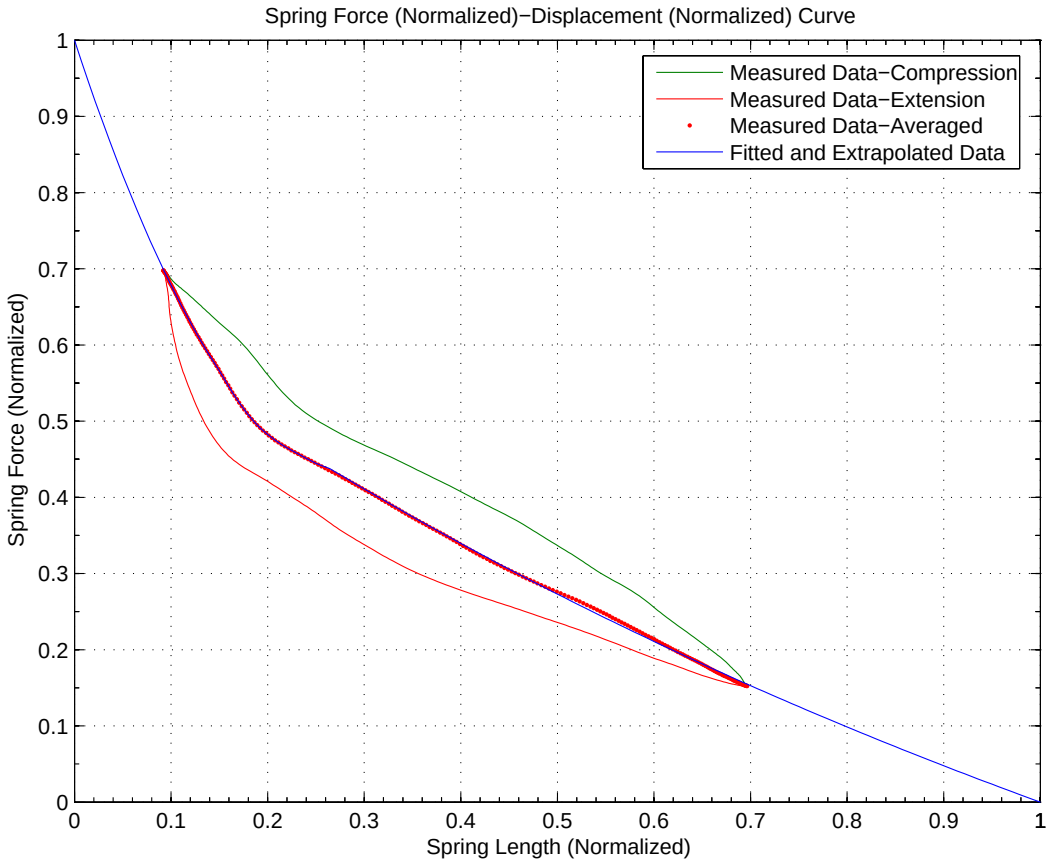

Figure 5.2: Force curves measured (compression, extension and averaged) along with the fitted and extrapolated curve

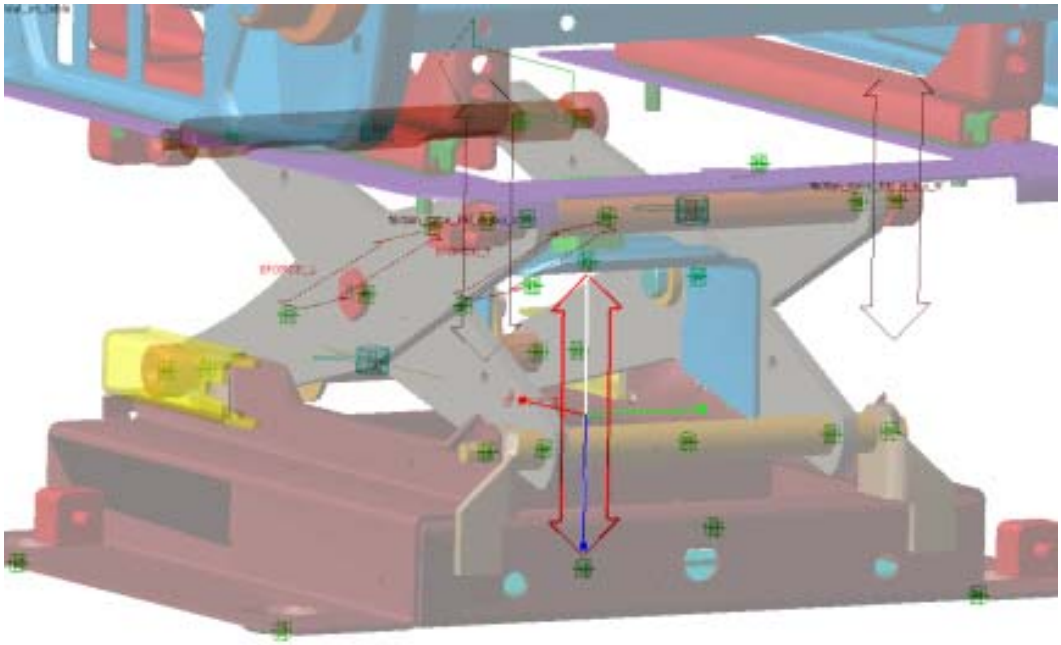

Figure 5.3: Airspring modeled in ADAMS/VIEW as an SFORCE

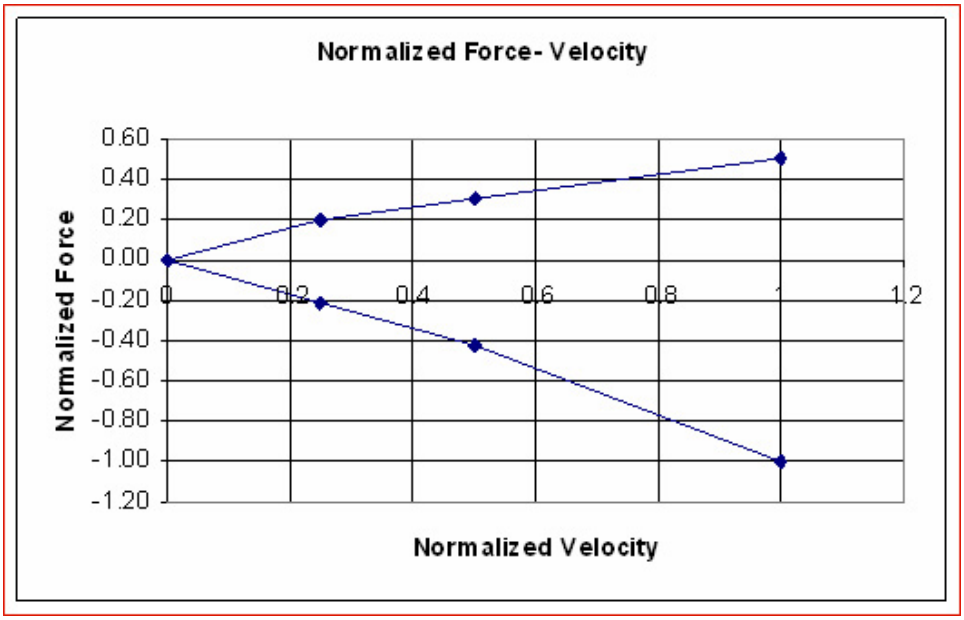

Figure 5.4: Normalized damper force-velocity curve

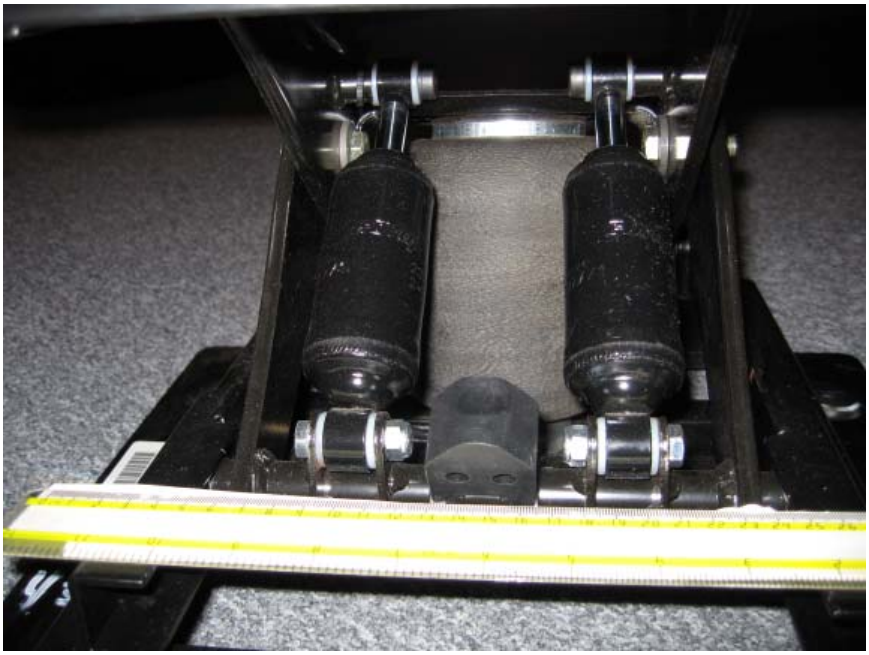

Figure 5.5: Damper as installed in the prototype

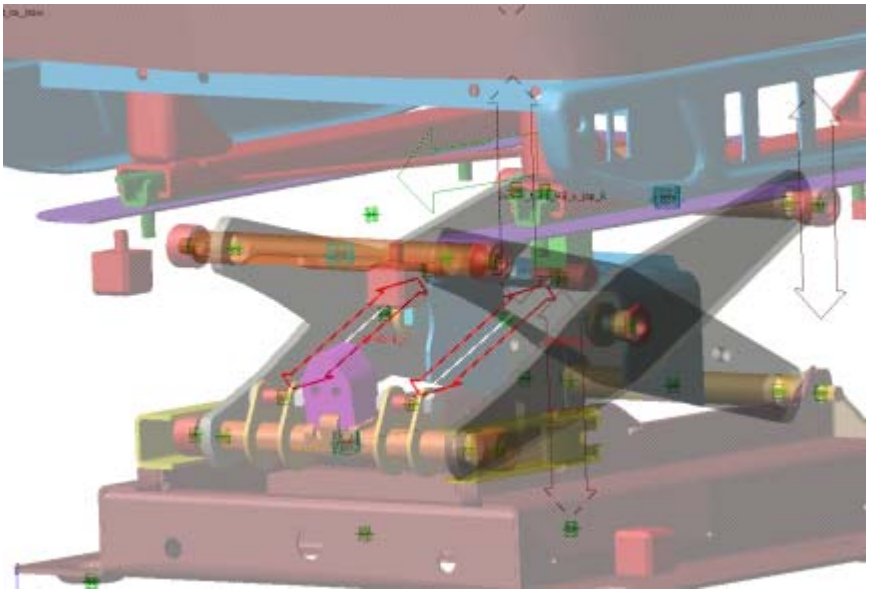

Figure 5.6: Damper modeled in ADAMS/VIEW as an SFORCE

using system identification techniques. For identifying the seat cushion system parameters, most of the literature [8, 19] report testing the seat cushion with a known mass resting on the cushion and then measuring acceleration across the cushion element. Using parametric system identification techniques the transfer function, which approximates the behavior of the system in a linear sense, is obtained. A similar, but slightly different, approach was used for modeling the seat cushion.

The random signal with frequency content from 0.5-20 Hz was used for this purpose. As mentioned in section 4.3, the Z -axis accelerations from the accelerometer 6 (refer Table 4.3) and that from the seat pad are first converted to displacements. These will respectively be the input and output of a transfer function, which represents the seat cushion. System identification was performed using Matlab's system identification toolbox [15]. The best fit model was determined based on magnitude of the output error and was ensured to have the best accuracy in the 4-8Hz range. The identified model is given by equation. 5.1. The comparison of measured and simulated output for the seat cushion are shown in Figure 5.7, while the frequency response of the transfer function is given by Figure 5.8.

$$\frac{Y(s)}{X(s)} = \frac{15.31s^3 + 1929s^2 + 45410s + 2.394E06}{s^4 + 23.58s^3 + 3468s^2 34080s + 2.38E06} \tag{5.1}$$

This, although not a very involved system identification process compared to that mentioned in [19], is a very convenient one for modeling in ADAMS.

ADAMS Implementation of the Seat Cushion In ADAMS there is a transfer function element which can be modeled by using the numerator and denominator coefficients of a continuous transfer function. Thus, using coefficients in Eq. 5.1, assigning input and output variables as the absolute displacement of the suspension top frame and dummy weight's reference point respectively, the cushion system transfer function was implemented [16]. Now if the suspension top frame's displacement is known, the transfer function gives the absolute displacement of the dummy weight. This forms only a part of the dynamic loop for the seat cushion system, as the inertial acceleration effects fo the dummy weight are not fed back to the suspension top frame as a reaction force. So an SFORCE element is inserted between the same two points which are used to reference the transfer function I/O. The function for this SFORCE will be of the form given by equation 5.2

$$ACCZ(DummyWeight) \cdot 75 + 75 \cdot 9.80665 \tag{5.2}$$

In 5.2 $ACCZ(DummyWeight)$ represents the Z-acceleration of the dummy weight, 75 the mass of the dummy weight and 9.80665 the acceleration due to gravity. This now completes

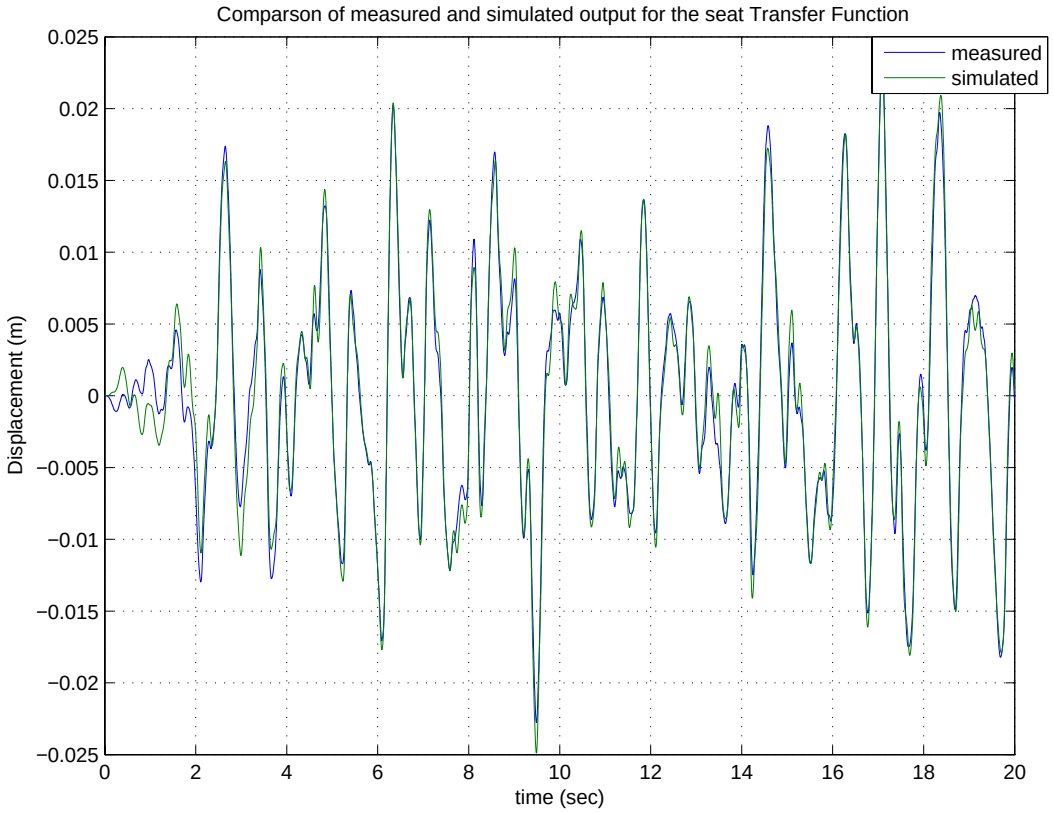

Figure 5.7: Comparison of measured and simulated output for the seat cushion

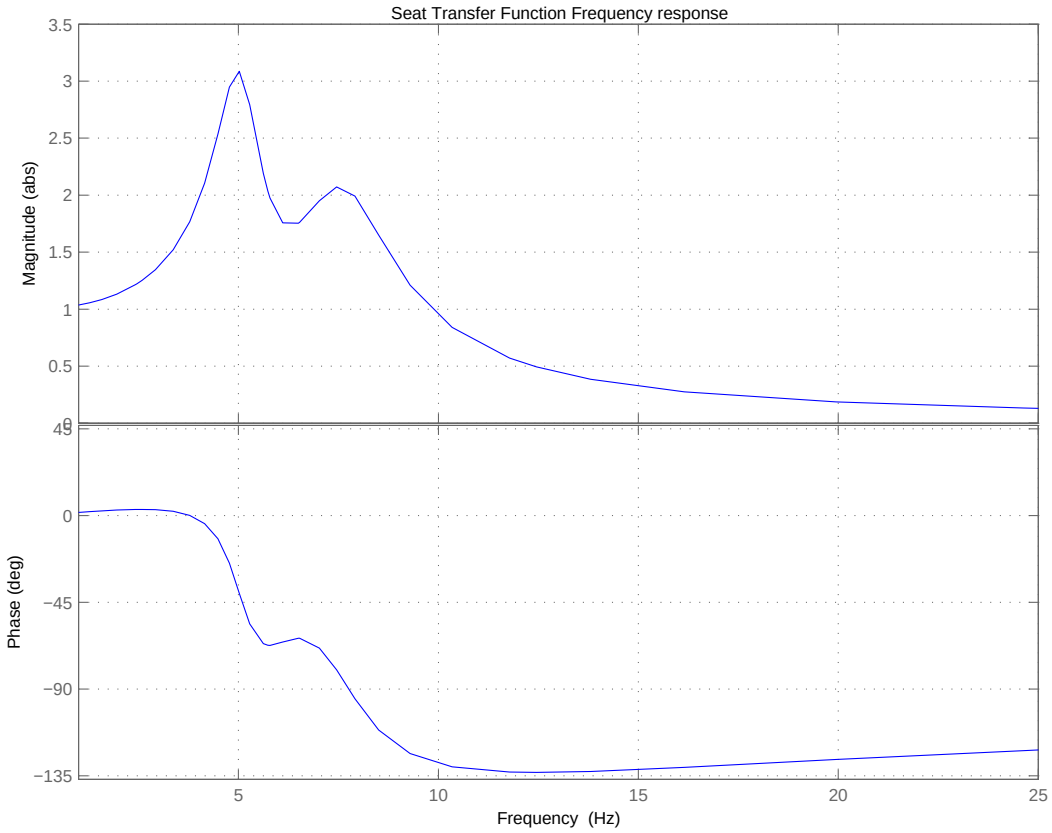

Figure 5.8: Frequency response for the seat cushion transfer function

Table 5.1: Friction parameters values

	Parameter	**Relative Motion**	**Value**
1	Steel-Steel (Static)	Sliding	0.08
2	Steel-Steel (Dynamic)	Sliding	0.05
3	Steel-Steel	Rolling	0.0005
4	Roller bearing	Rotation	0.0011

the dynamic loop where the suspension top gets the reaction forces produced by the dummy weight's acceleration. This interaction is depicted by Figure 5.9

5.5 Friction Modeling

Modeling the friction in the model has been addressed at two main locations.

- The center pivot of the suspension cross arms
- Roller bearings. Figure 5.10

These locations have been noted to have the most normal reaction and relative motions, and therefore are the dominant contributers to friction in the system. The standard values for static and dynamic friction for the steel-steel material pairs and those for roller bearing friction have been referenced for web literature [7]. Table 5.1 gives the friction parameters used in the model. The details of the friction subroutine in ADAMS to calculate the friction forces can be found in the ADAMS documentation [16].

5.6 MTS 6-Axis Simulator

The MTS 6-axis simulation table model was already developed by the National Seating and was imported into ADAMS as ADAMS modeling database file. At the location of the three accelerometers, ACCM01, ACCM02 and ACCM03 (refer table 4.3) the markers for input motion were modeled. The details are provided in section 5.7. The markers served as the points of the input vibration motions. For the validation of the simulator alone, the markers were placed as mentioned in section 4.1.

5.7 Assembly of Seat and Simulator Models

The seat model was merged into the table model with the seat base interacting with the table surface through a fixed joint (lock joint). A fixed joint constraints all the relative degrees of freedom. Figure 5.11 shows the assembled simulator and seat models.

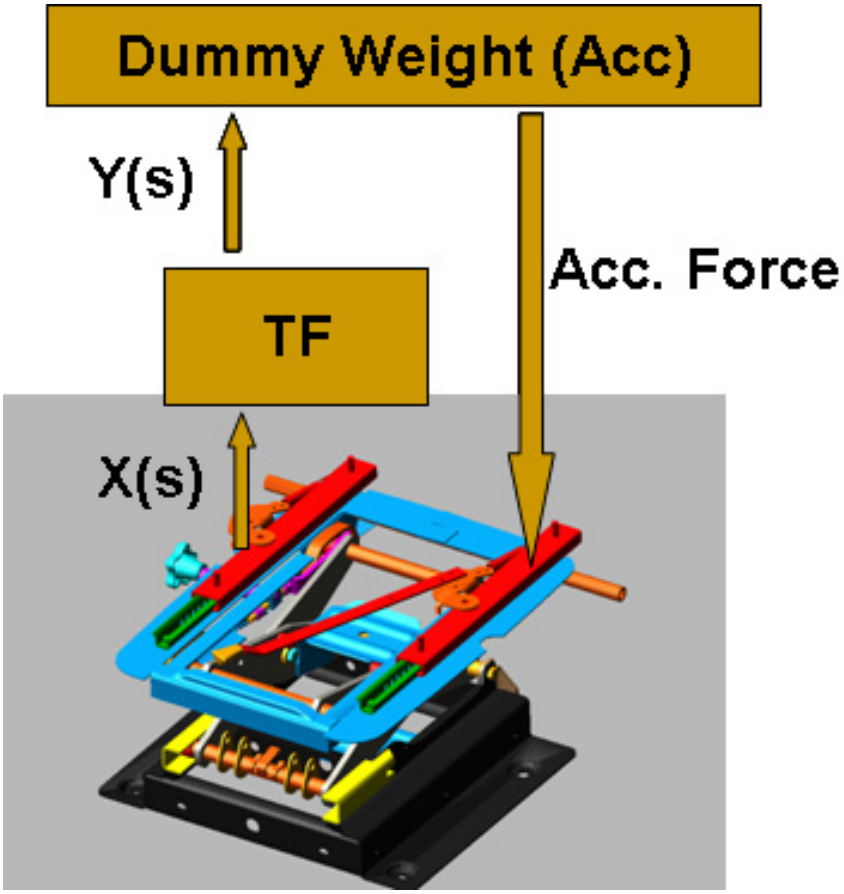

Figure 5.9: Representation seat cushion transfer function implementation in ADAMS

Figure 5.10: Location of roller bearing elements for friction force application

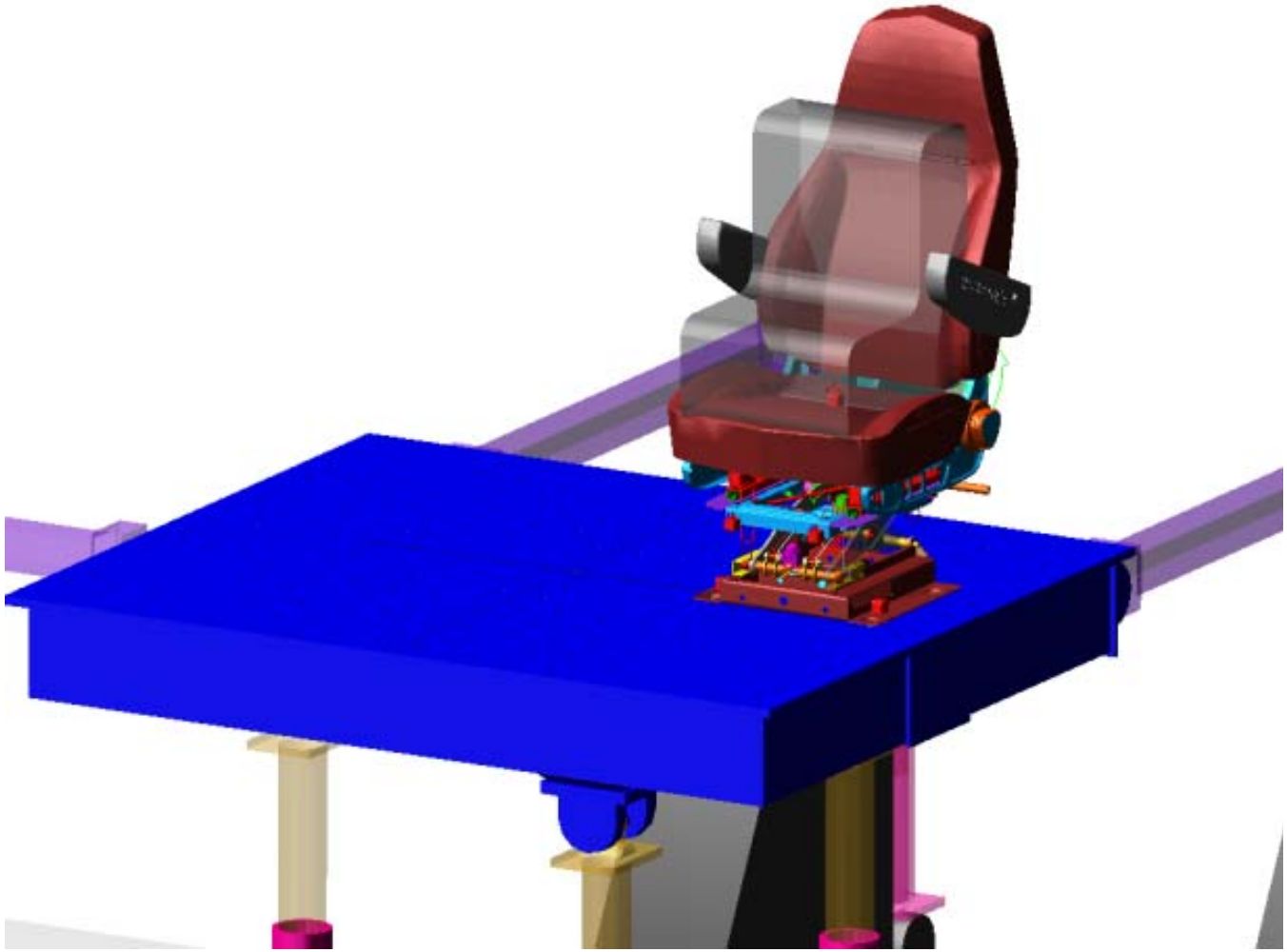

Figure 5.11: MTS 6-Axis Simulator modeled in ADAMS/VIEW

Table 5.2: Motion input to ADAMS model: accelerometers and axes

Accm No.(test)	**Accm No.(Model)**	**Motion Axes**
1	3	X,Y,Z
2	2	Z
3	1	X,Z

The accelerometers markers were fixed at exactly (with 5mm precision) the same locations as that on the prototype. Six motion generators were fixed to the three accelerometers at the base of the seat frame. The orientations are given in Table 5.2.

With the whole system setup, the model is now ready for simulations using the various inputs.

5.8 Simulation Setup

There are two possible environments to run the simulations:

- ADAMS/VIEW: Import the input signals to drive the motion generators in the form of displacement, velocity or acceleration splines as a function of time and allow the simulation to run in ADAMS. Then export the result set to Matlab where it can be analyzed using the various evaluations methods.

- ADAMS/MATLAB-SIMULINK Cosimulation: ADAMS/Controls is a plugin that allows the ADAMS/VIEW dynamic system to be exported to MATLAB/SIMULINK as a Simulink block. In this case Simulink controls the simulation time and feeds the input signals to the ADAMS block. ADAMS runs its dynamic solver behind the Simulink mask and continuously outputs the selected variable states to Matlab. Figure 5.12 shows the Simulink model of the cosimulation setup.

Both these configurations have their advantages and disadvantages. When the simulations are run by ADAMS, the inputs and the outputs need to be imported and exported respectively to Matlab for each run. Although ADAMS postprocessor is good for graphing the data, Matlab is better equipped for analyzing the data. However ADAMS has its own advantages in terms of computations speed as the ADAMS solver is C++ based and is very efficient. It is also easy to fine tune the parameters between runs, to setup optimization runs and to perform DOE. On the other hand if analyzing the model is the sole purpose of the simulation the ADAMS-SIMULINK cosimulation environment is convenient as Simulink controls the entire simulation from processing the raw data to analyzing the results. So it can be inferred that the ADAMS as a standalone system is better in design and model tuning phase while cosimulation system is better the analysis phase.

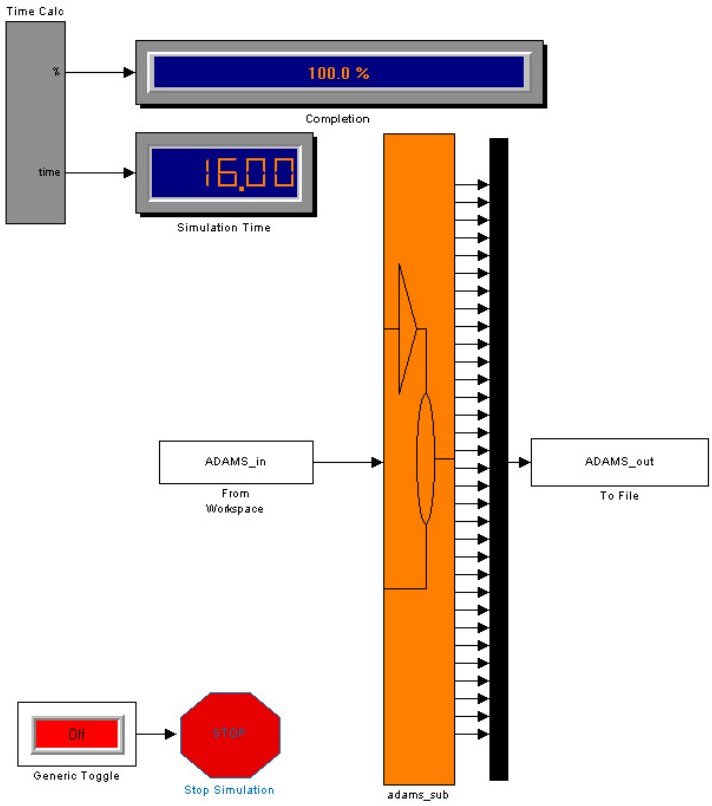

Figure 5.12: Cosimulation system Simulink model

Chapter 6

Results

This chapter provides a collection of the results for the various tests and simulations. The results mostly comprise of plots of the tested and simulated acceleration values in the time and frequency domains. These results help in providing important insights about the behavior of the model, its usability for whole body vibration evaluations and also offer direction for future developments. According to the three test sessions, this chapter is also divided into results for:

- MTS 6-axis simulator model
- Airspring model
- Seat model

6.1 MTS 6-Axis Simulator

The simulator model contains only rigid bodies connected by joints and no force elements are present. The purpose of testing the model did not involve determining the force required by the actuator to produce the required motion but only verifying whether the displacement at the actuator produced the required acceleration at the surface and vice versa. This means that technically it was a kinematic model and simulation rather than kinetic. The displacements at the actuators are used as the validation parameters, as their values during testing are available directly from the feedback LVDTs.

For the validation of the simulator model the approach used was as follows

- Convert the acceleration signal from the surface accelerometers to displacement.
- Input this displacement signal to the point motion generators in the ADAMS model.

- Validate the model performance by comparing the displacement produced at the six actuators in the model to that measured by the six corresponding LVDTs on the actual simulator.

This selection of input and output parameters was done so that two objectives can be achieved in one process:

1. Validation of the simulator model: The results directly established the accuracy of the 6-axis simulator model.

2. Validation of the data processing methods: At the start of the study it was not clear whether the process of collecting the acceleration data and then using the various data processing techniques mentioned in Chapter 3 would accurately reproduce the displacements. Therefore if the inputs and outputs are as mentioned above, for the displacements at the actuators in the simulations to match those measured during the test, both the model and the data processing methods should be accurate.

Thus both the model and the data processing methods can be validated. The 0.5-20Hz random signal was used in this verification process. The plots showing the comparison of the tested and simulated actuator displacement are shown in Figures 6.1 to 6.6.

6.2 Airspring Model

The airspring is modeled in ADAMS using the measured data and cubic spline interpolation as mentioned in section 4.2. As the internal damping in the spring is modeled by a viscous damper (a linear element) it will not represent the accurate internal damping at all the frequencies. Accordingly, the damping coefficient value was tuned to give good results at the important frequency of 5 Hz. Figure 6.7 shows the comparison of the simulated and tested force values at a frequency of 5 Hz.

It can be seen from Figure 6.7 that the airspring model behavior matches closely that of the actual airspring around the 5Hz region which is the critical frequency range when considering spine vibrations.

6.3 Seat Model

The results are presented in two parts based on the type of the input, sinusoidal and random. Comparison between test and simulated values has been done in the time and frequency domains as well as using whole body vibrations evaluation parameters:

1. Peak

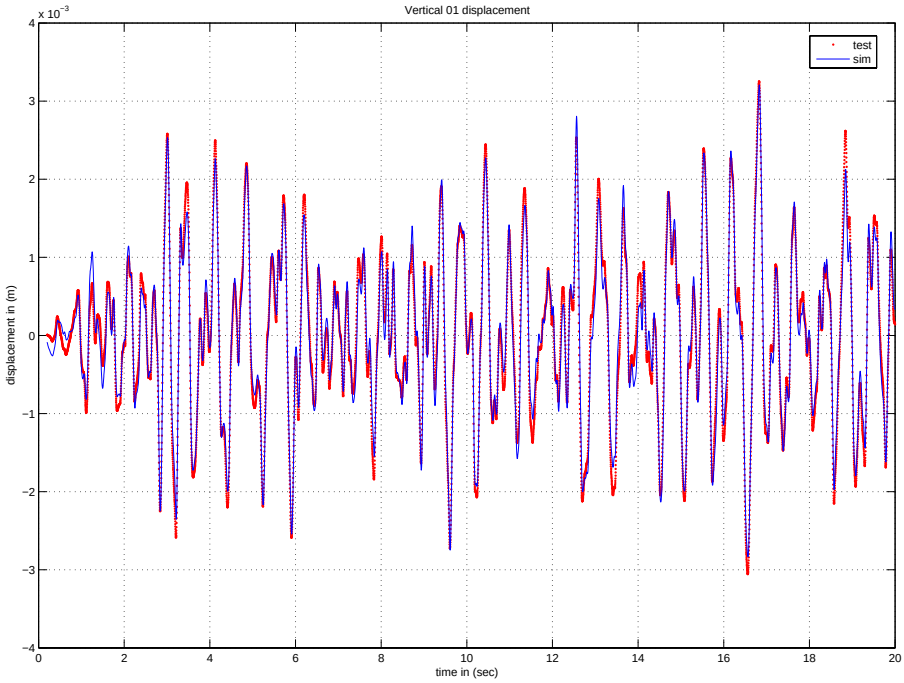

Figure 6.1: Displacement results for Vertical Actuator 1: 0.5-20hz random input

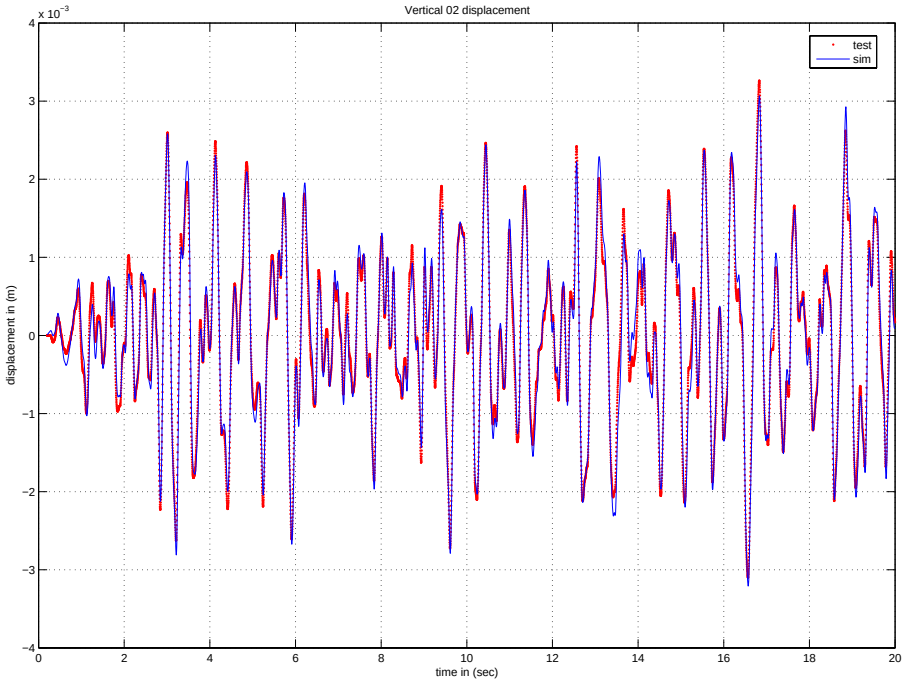

Figure 6.2: Displacement results for Vertical Actuator 2: 0.5-20hz random input

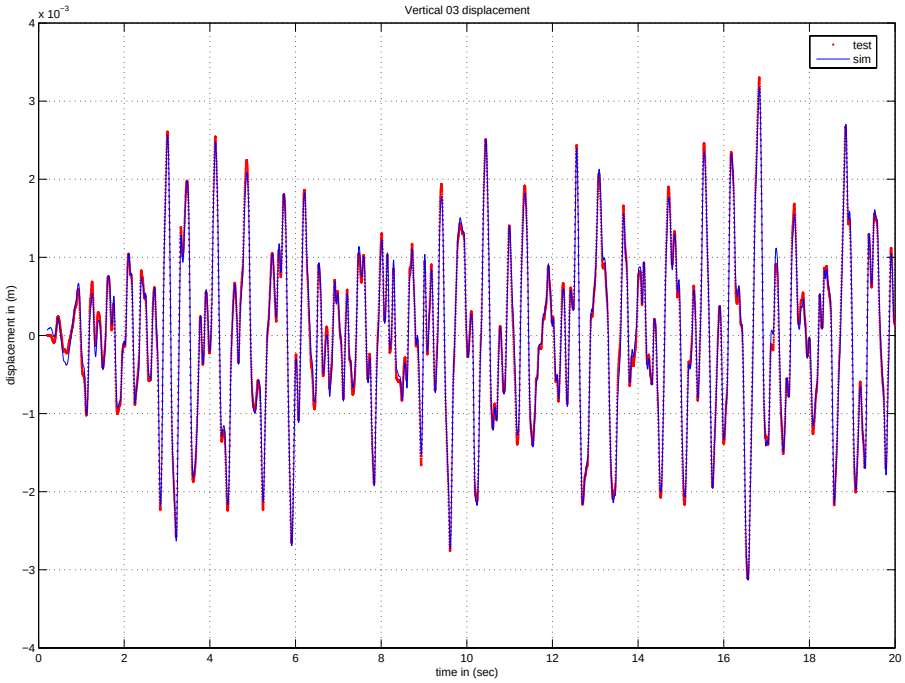

Figure 6.3: Displacement results for Vertical Actuator 3: 0.5-20hz random input

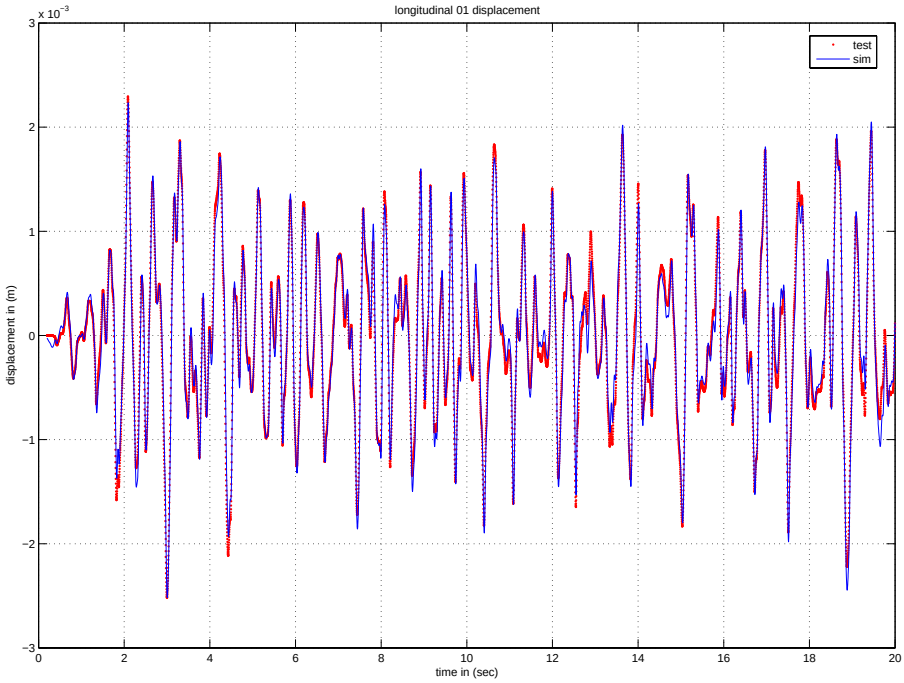

Figure 6.4: Displacement results for Longitudinal Actuator 1: 0.5-20hz random input

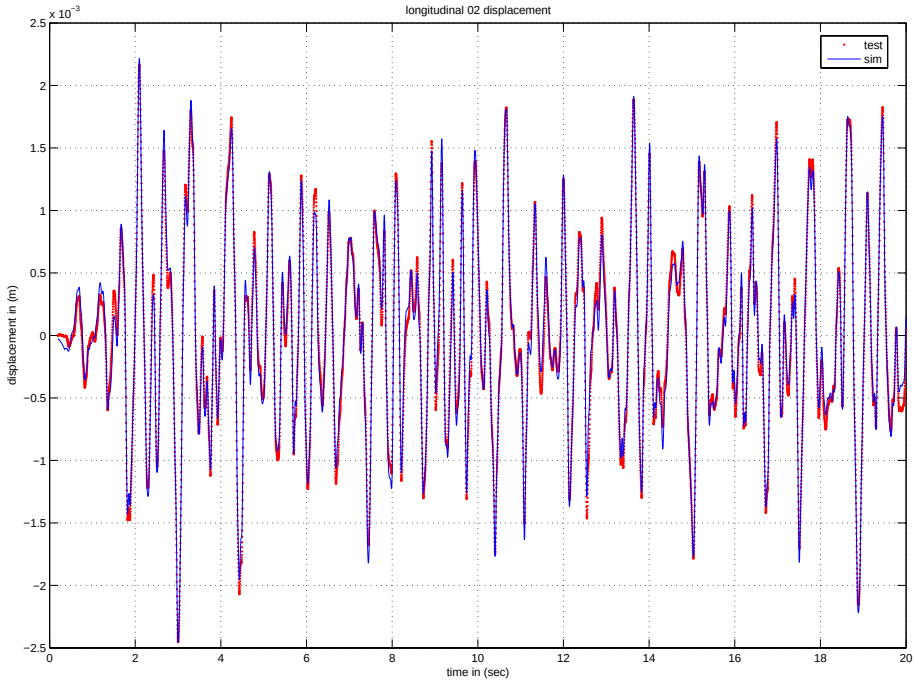

Figure 6.5: Displacement results for Longitudinal Actuator 2: 0.5-20hz random input

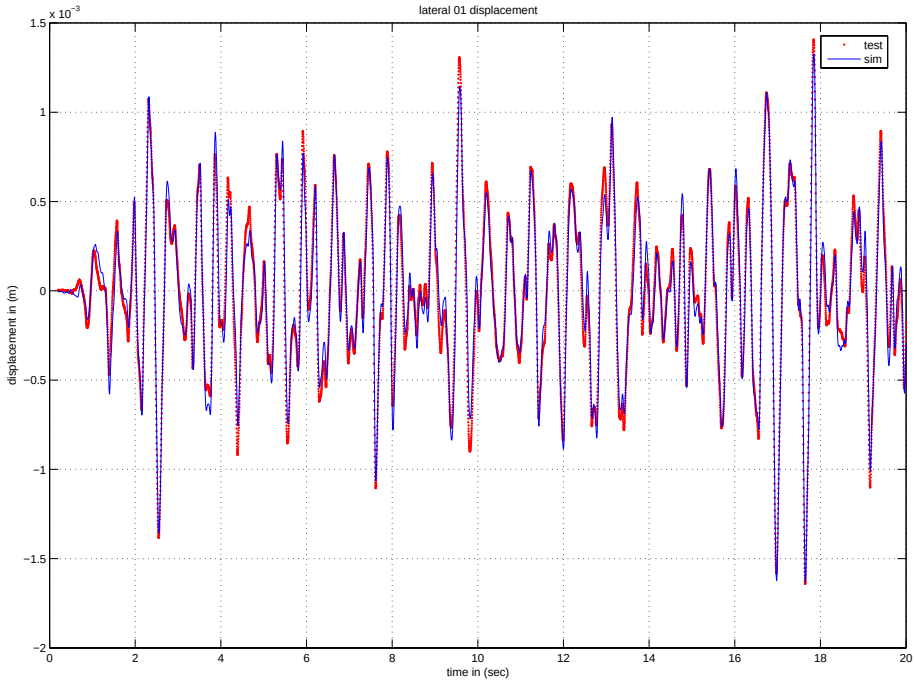

Figure 6.6: Displacement results for Lateral Actuator 1: 0.5-20hz random input

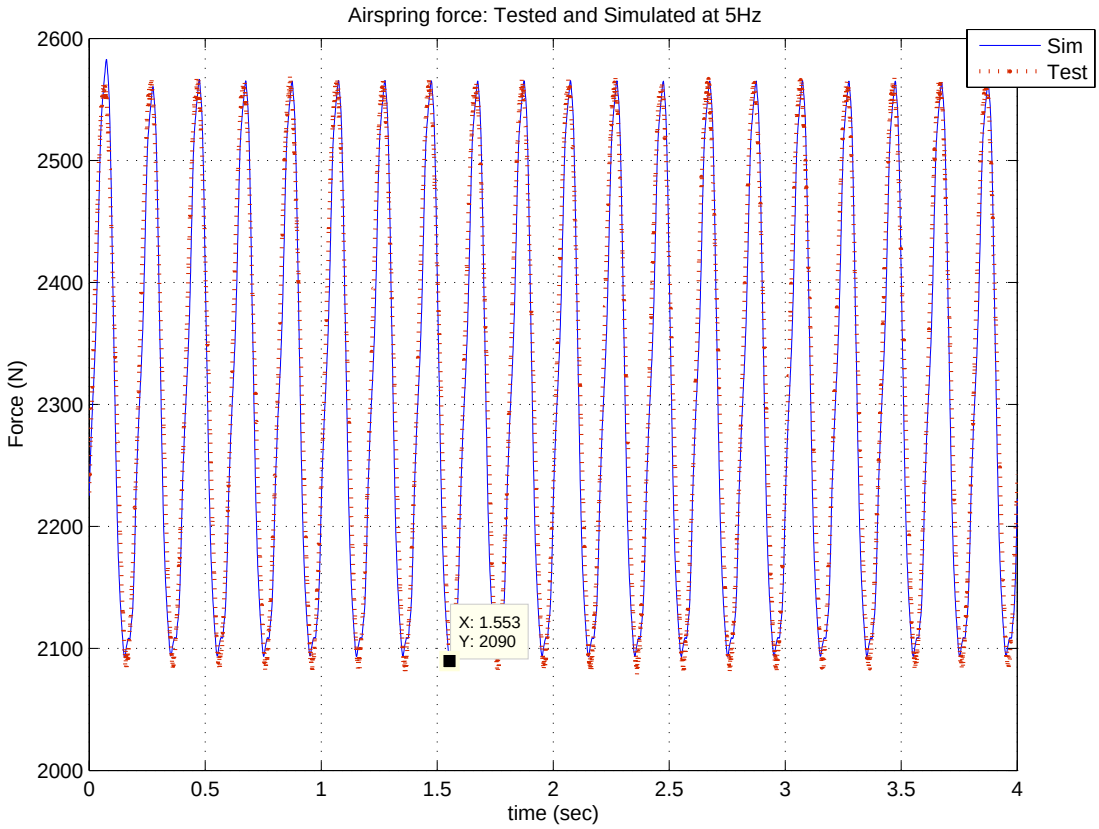

Figure 6.7: Airspring force: Tested and Simulated at 5 Hz

2. RMS
3. RMQ
4. Crest Factor
5. VDV
6. eVDV

Peak value Peak Value is the maximum deviation of the time series from the mean value of the series.

Root-Mean-Square: RMS The RMS value of the time series is given by

$$RMS = \left[\frac{1}{N}\sum x^2(i)\right]^{\frac{1}{2}} \tag{6.1}$$

For a sinusoidal motion of amplitude, A, the RMS value is $2^{-1/2}A$

Root-Mean-Quad The root-mean-quad of a time series is given by

$$RMQ = \left[\frac{1}{N}\sum x^4(i)\right]^{\frac{1}{4}} \tag{6.2}$$

For a sinusoidal motion of amplitude,A, the RMQ value is $(3/8)^{1/4}A$

Crest Factor The crest factor is given by the ratio of the peak value to the RMS value of the time series.

$$\text{Crest factor} = \frac{Peak}{RMS} \tag{6.3}$$

For a sinusoidal signal the crest factor is $1/\sqrt{2}$.

Vibration Dose Value: VDV The vibration dose value of a time series is given by

$$VDV = \left[\frac{T_s}{N}\sum x^4(i)\right]^{\frac{1}{4}} \tag{6.4}$$

For a sinusoidal motion of duration T_s and amplitude A, the VDV is $(3/8)^{1/4}A \cdot T_s^{1/4}$.

Estimated Vibration Dose Value: eVDV This value is relevant for signals with crest factors less than 6 (normal VDV is valid for any crest factor). The eVDV value of a time series is given by

$$VDV = [(1.4RMS)^4 \cdot T_s]^{1/4} \tag{6.5}$$

The use of these parameters for whole body vibration evaluations have been introduced by M. J. Griffin [4].

6.3.1 Response to Sinusoidal Inputs

To get an idea about the seats response to steady-state sinusoidal input, the results for the 1Hz, 5Hz and 8Hz inputs have been presented here. These frequencies have been chosen to be the focus of the discussion as 1 and 8Hz represent the outer bounds for the range of frequencies of interest and 5Hz is approximately the frequency which has been noted [4]to cause the most discomfort and back problems. The results for the z-axis accelerations for accelerometer-6 (uniaxial attached to the seat frame between airspring and cushion) and the seat pad accelerometer are included. These accelerations are representative of the vibration motion of the seat frame just below the cushion and that at the cushion and dummy-weight interface. They give a good understanding about the behavior of the suspension system and the cushion. Figures 6.8 to 6.19 show the plots for the 1,5 and 8Hz input signals in the time and frequency domains.

It can be observed that the since the model was tuned to perform the best at and around the 5hz region, the agreement between the tested and simulated values is the best in that frequency neighborhood. Figures 6.20 and 6.22 present the comparison of the whole body vibration parameters for the tested and simulated analysis, while Figures 6.21 and 6.23 present the $\%error$ between the tested and simulated values. For calculating the error the tested values are used as the reference. Positive $\%error$ bars indicate overestimation of values by the simulations and vice versa. From these plots it can be seen that the simulated values are within 5% error in the 5Hz frequency region. As the frequency goes on increasing the deviation of the model goes on increasing.

6.3.2 Response to Random Inputs

Here, similar to section 6.3.1 the results for the accelerometer-6 and seat pad for the z-direction are provided. The results are in both the time and frequency domains. The time domain plots do not make much sense visually, as it can be seen from section 6.3.1 that, the model's response is not accurate at all the frequencies. However, the frequency domain plots provide a much better understanding of the model's behavior. Figures 6.24 and 6.25 show the time domain plots along with the whole body vibration evaluation parameters

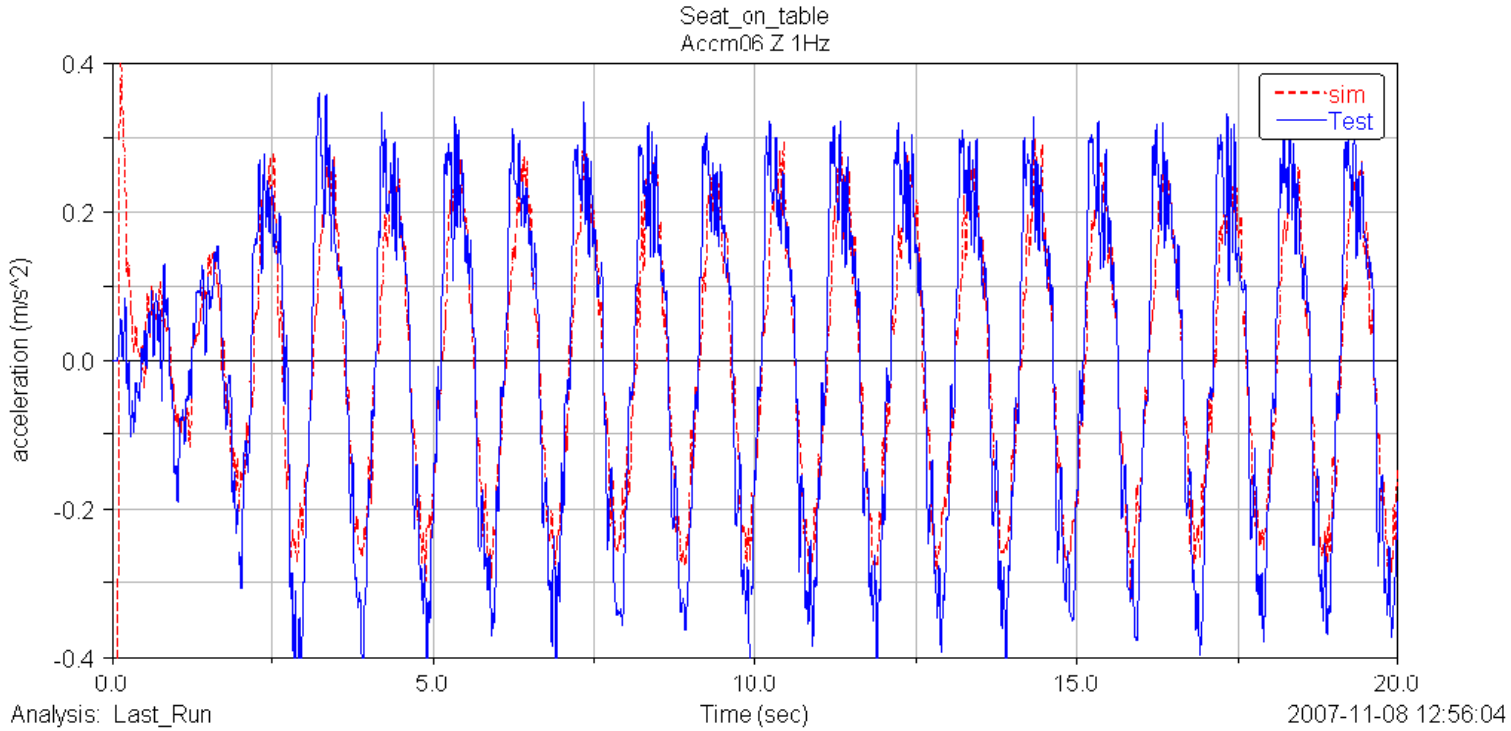

Figure 6.8: Results: Accelerometer-06 Z 1Hz time plot

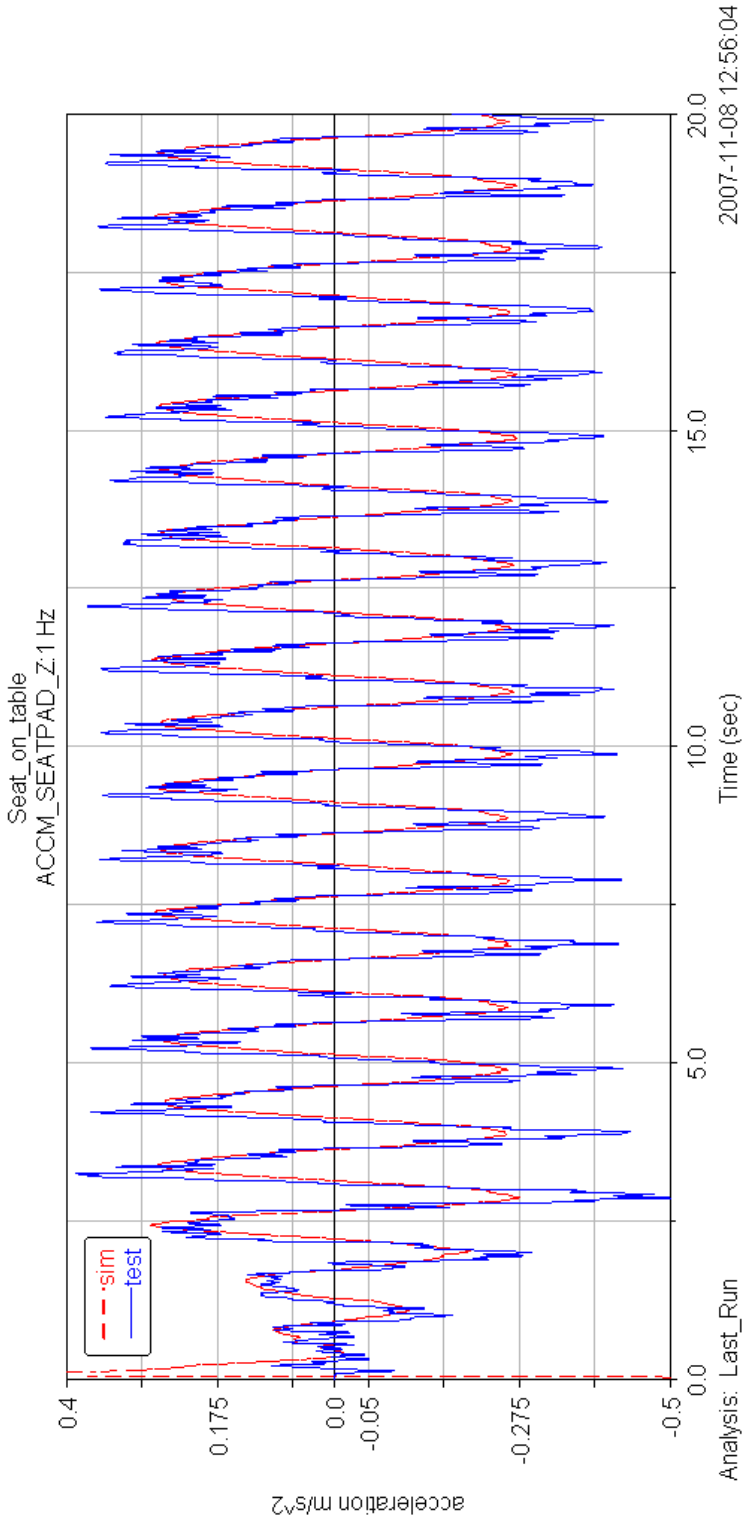

Figure 6.9: Results: Accelerometer-SP Z 1Hz time plot

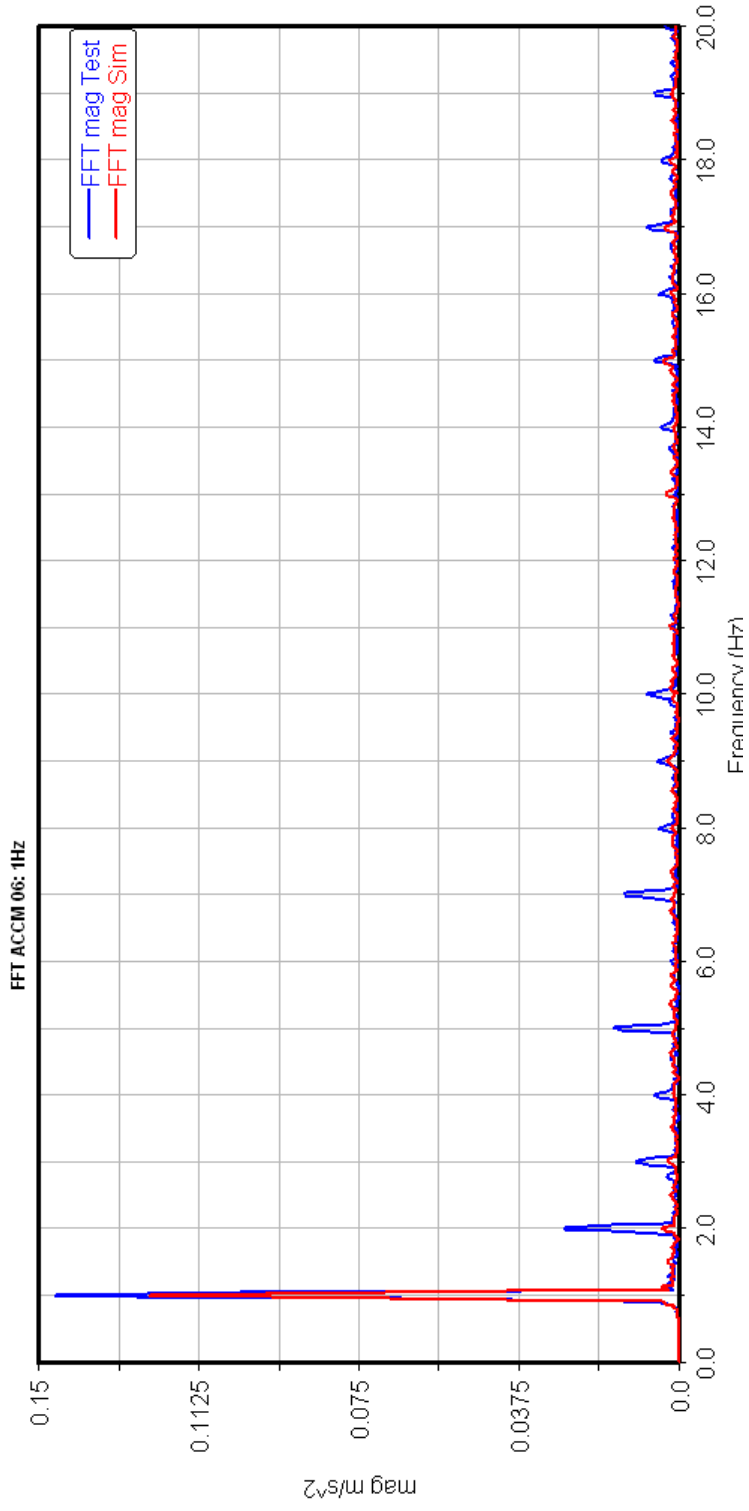

Figure 6.10: Results: Accelerometer-06 Z 1Hz fft plot

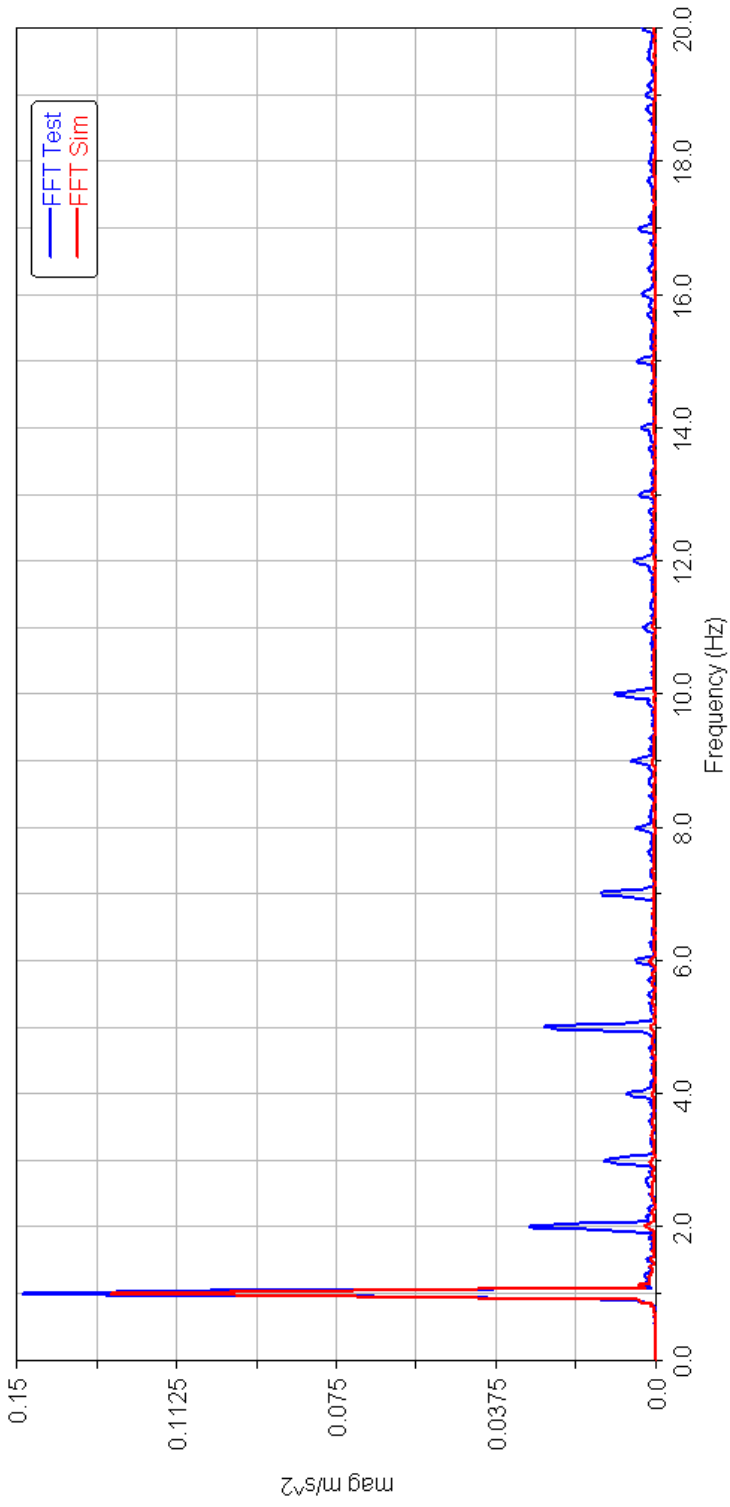

Figure 6.11: Results: Accelerometer-SP Z 1Hz fft plot

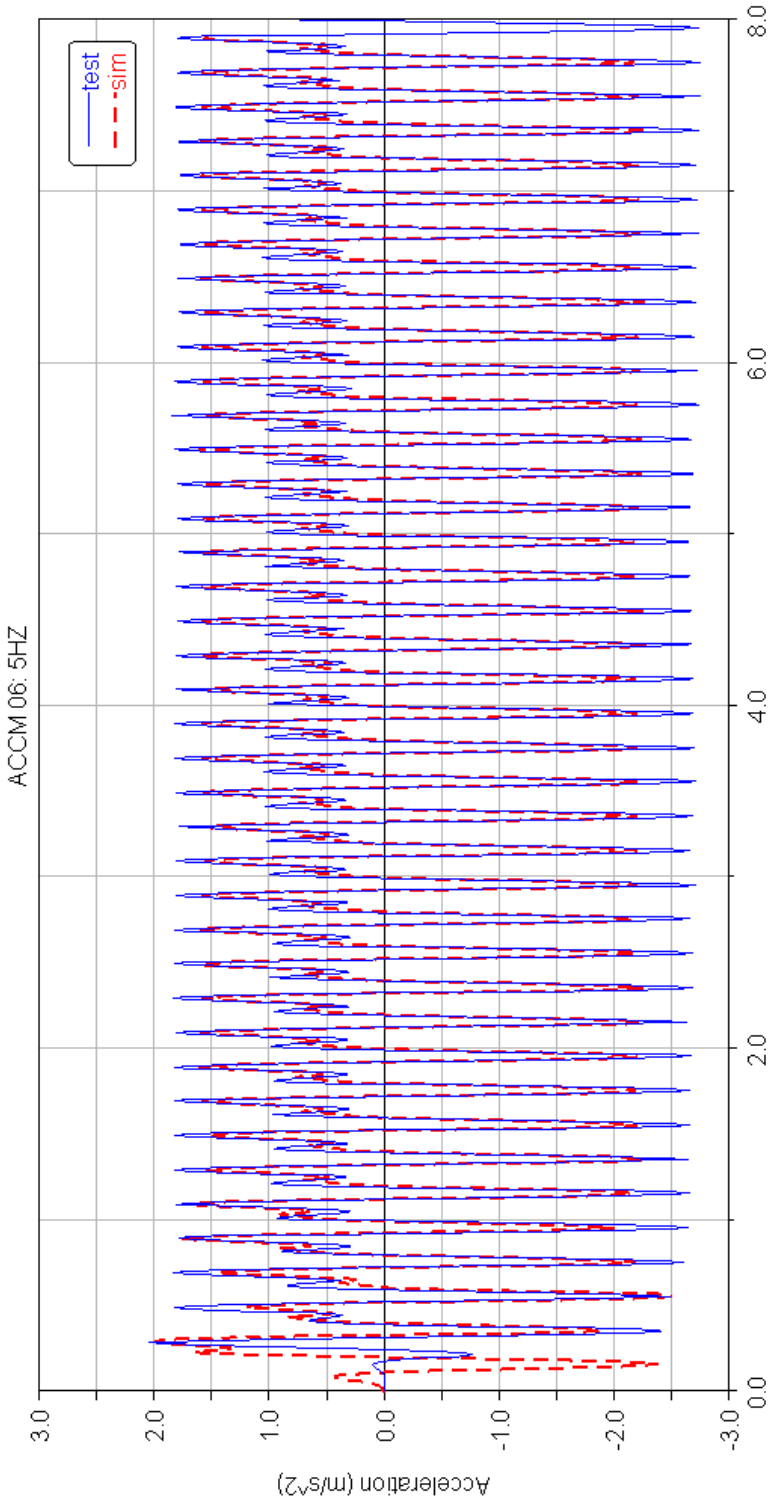

Figure 6.12: Results: Accelerometer-06 Z 5Hz time plot

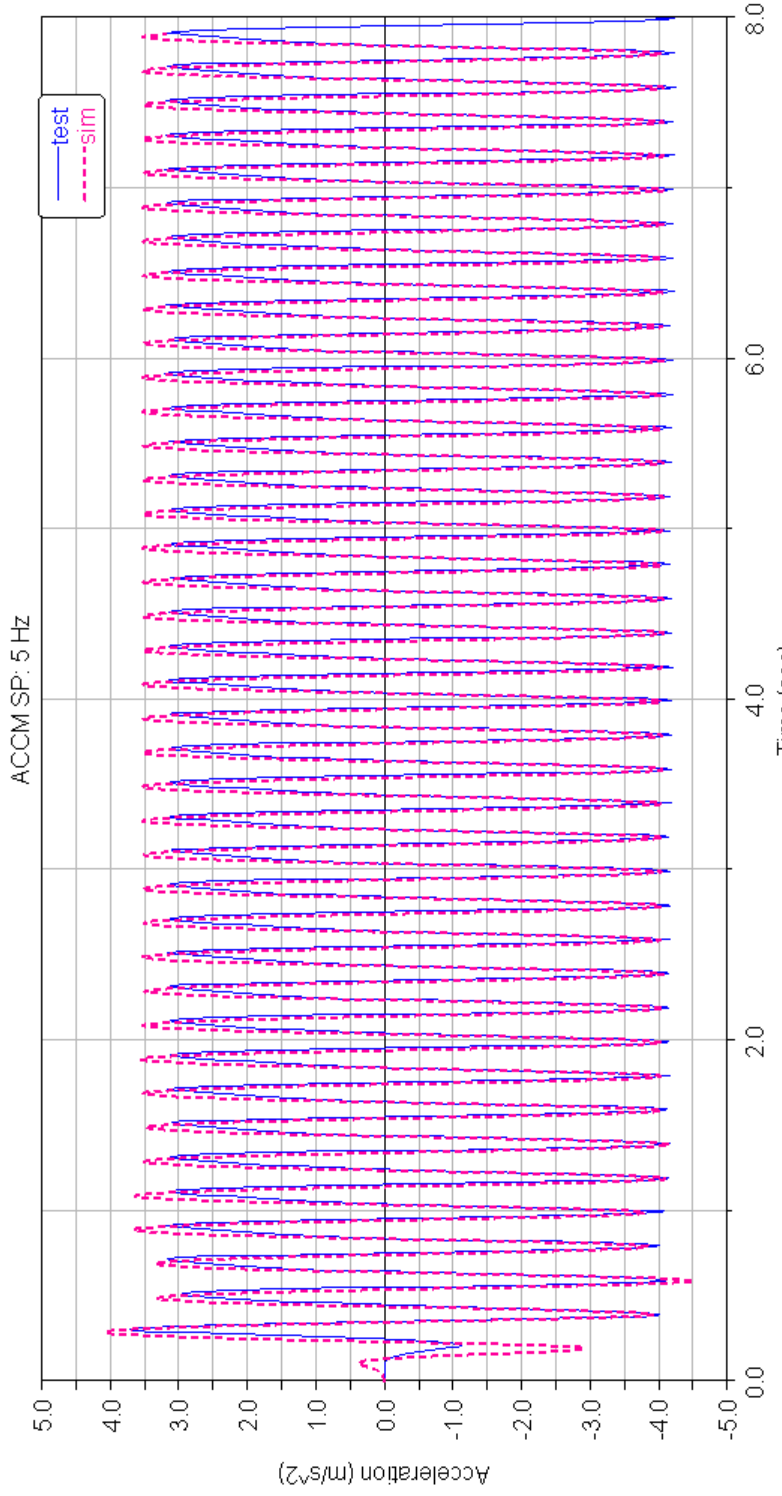

Figure 6.13: Results: Accelerometer-SP Z 5Hz time plot

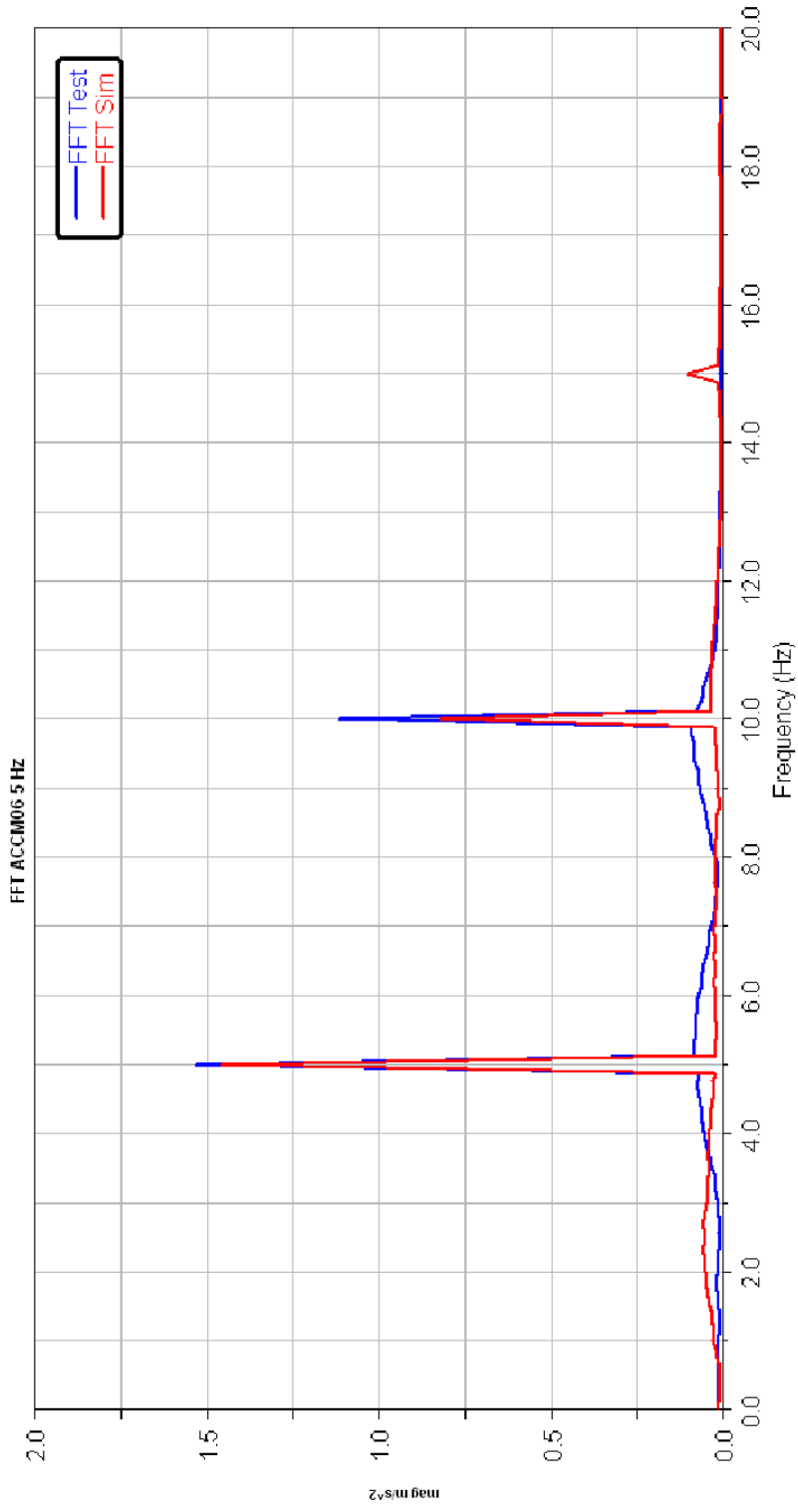

Figure 6.14: Results: Accelerometer-06 Z 5Hz fft plot

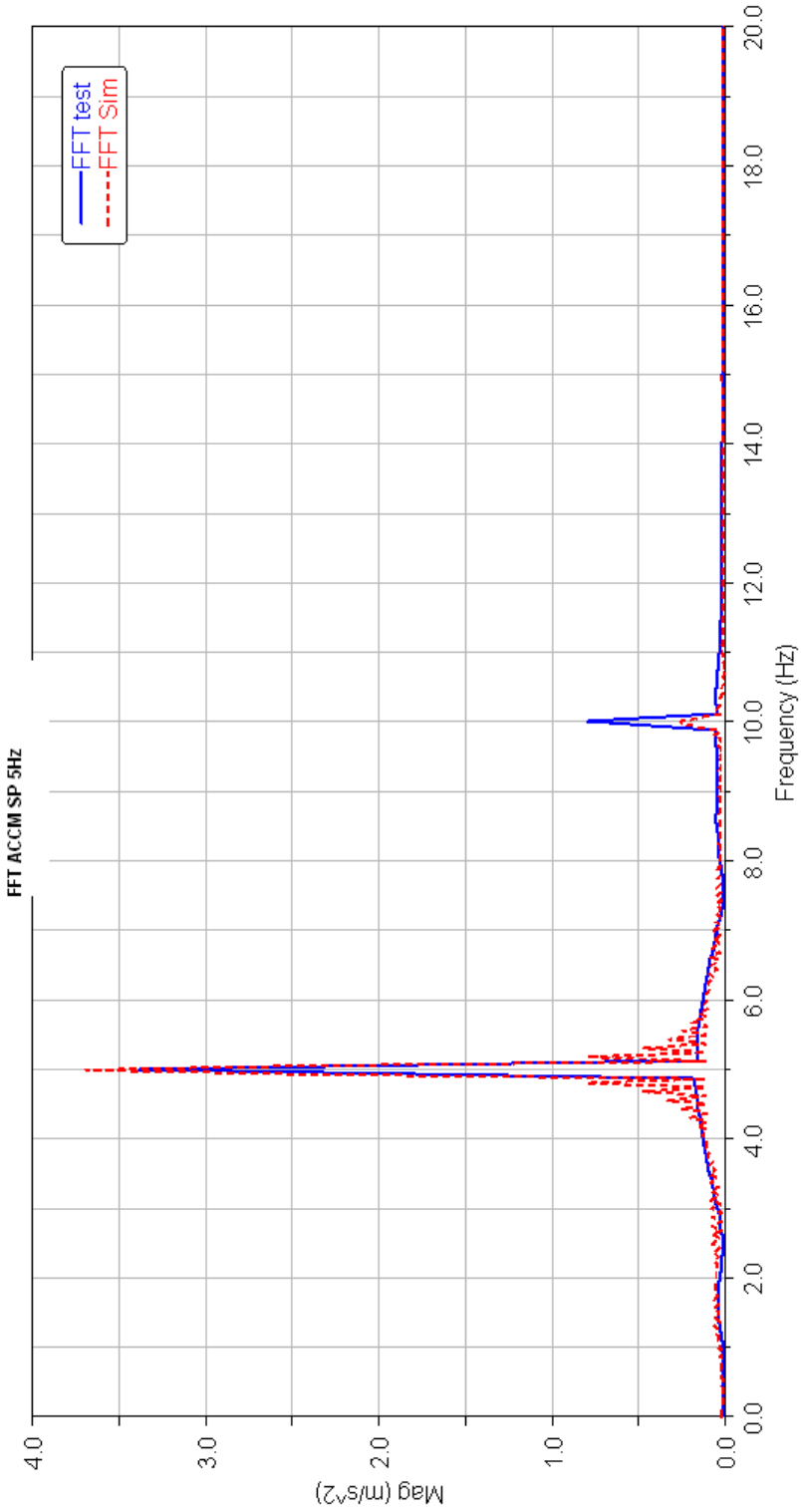

Figure 6.15: Results: Accelerometer-SP Z 5Hz fft plot

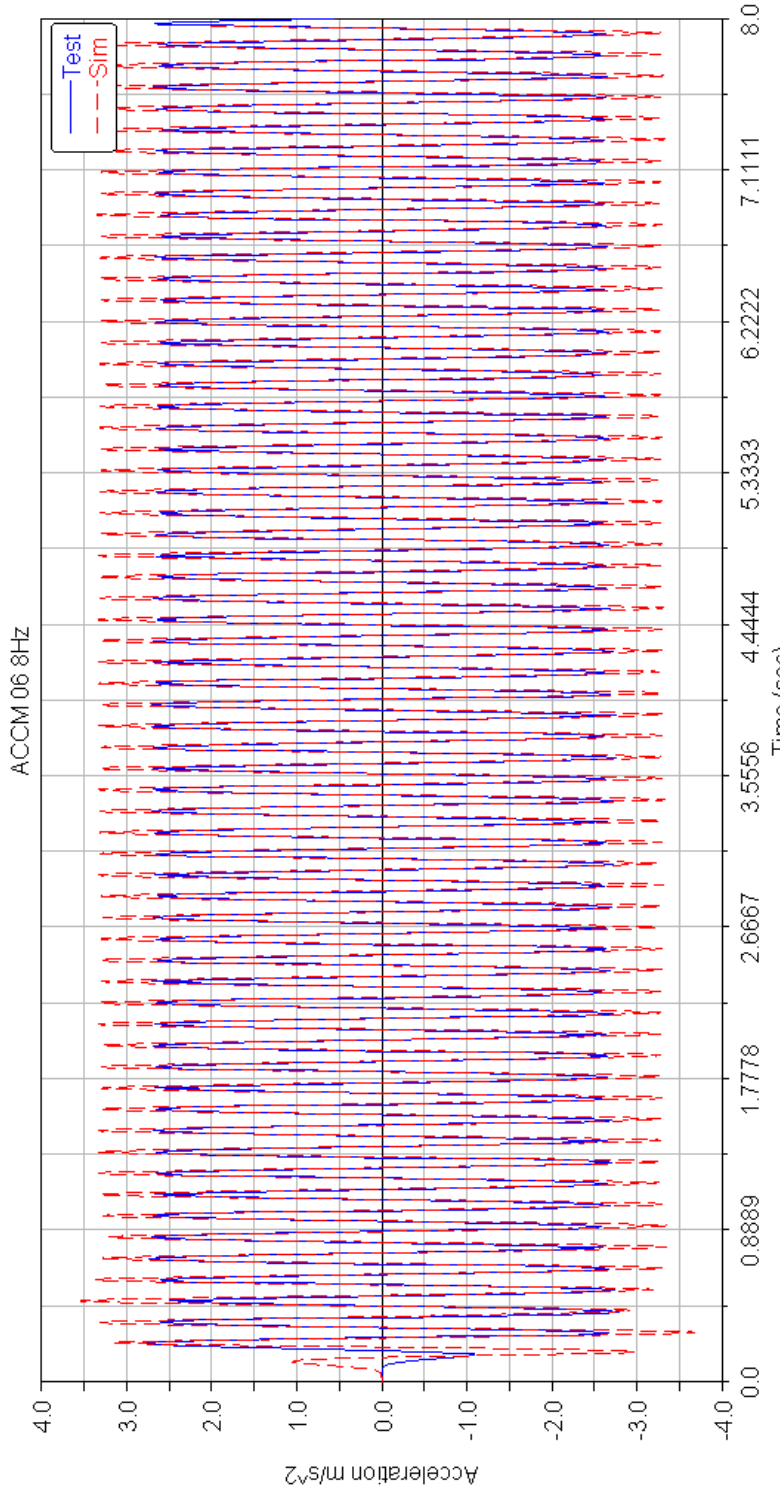

Figure 6.16: Results: Accelerometer-06 Z 8Hz time plot

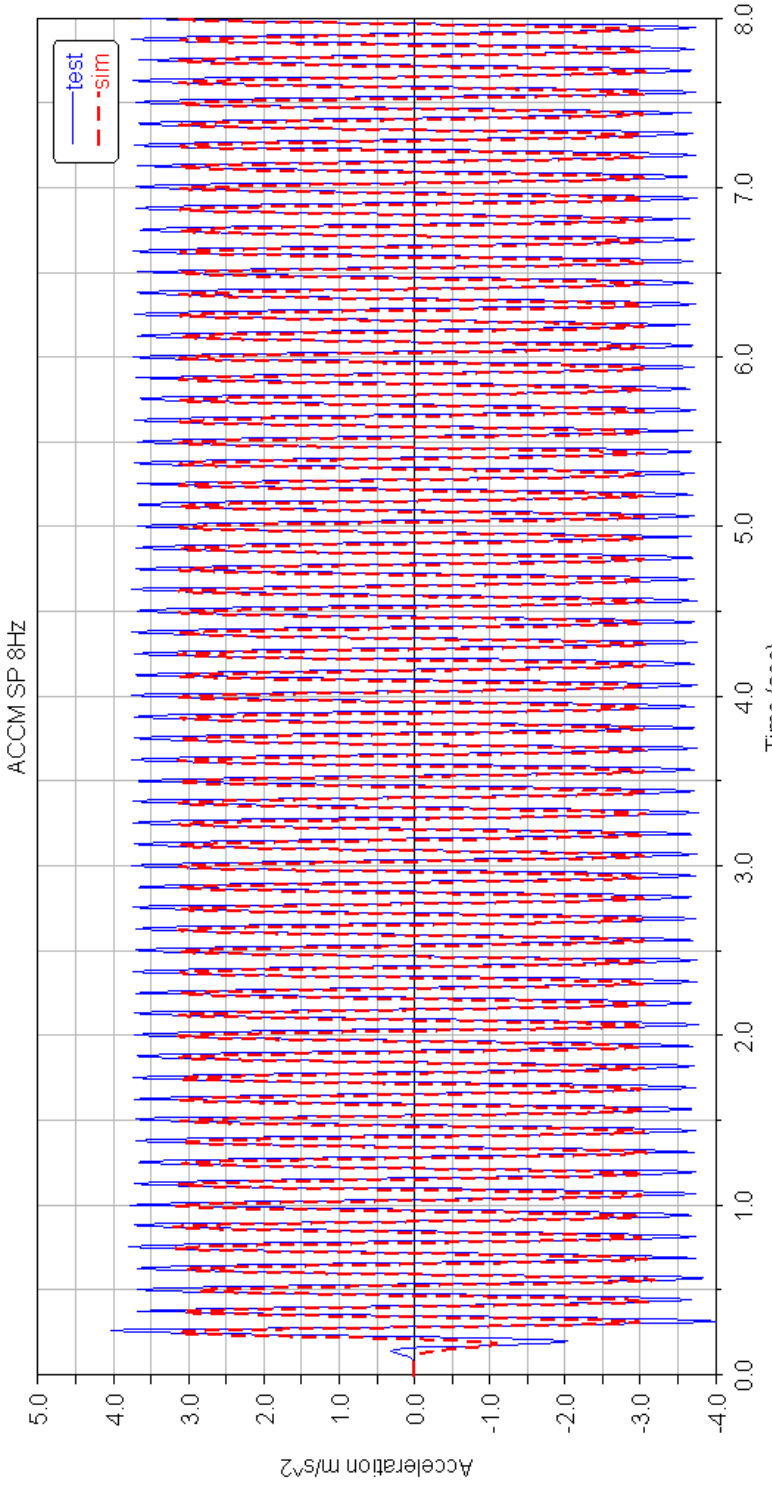

Figure 6.17: Results: Accelerometer-SP Z 8Hz time plot

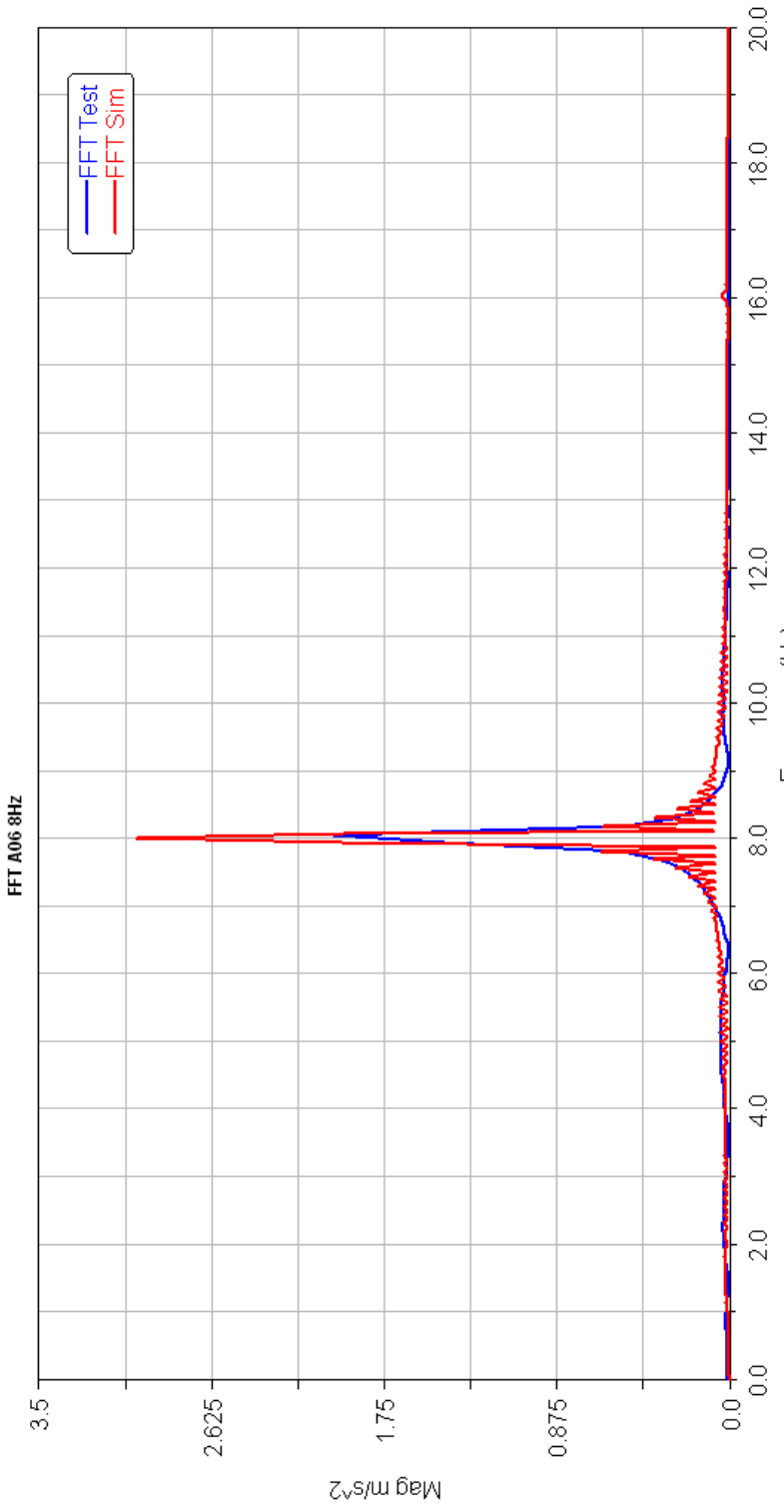

Figure 6.18: Results: Accelerometer-06 Z 8Hz fft plot

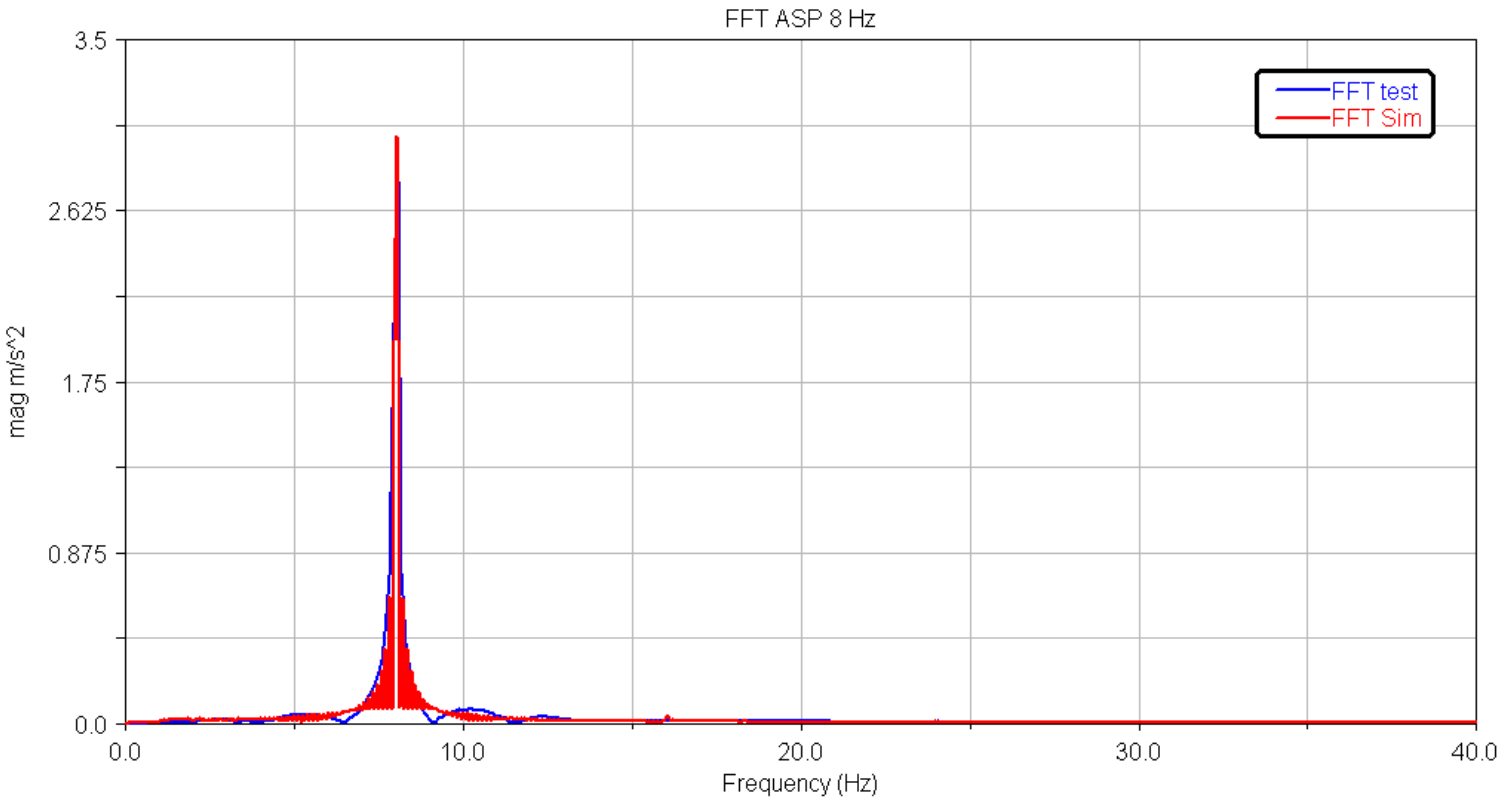

Figure 6.19: Results: Accelerometer-SP Z 8Hz fft plot

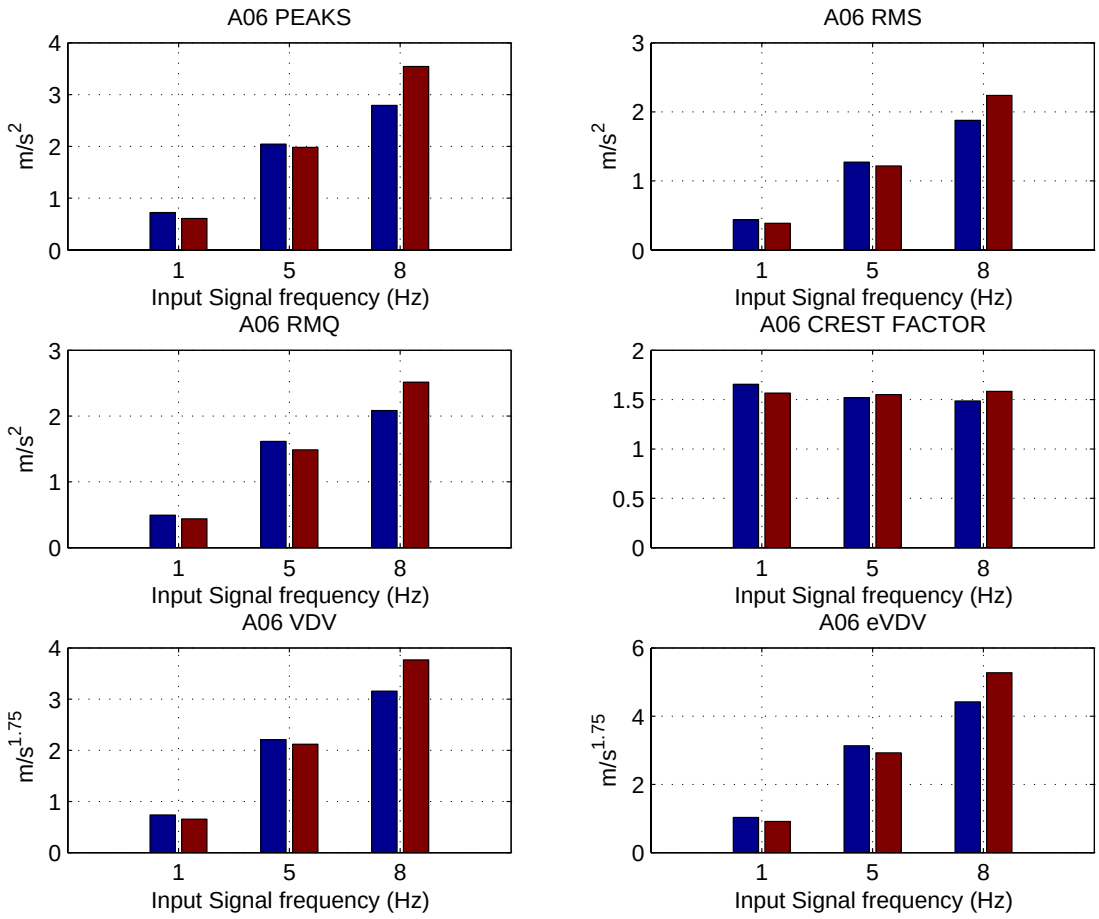

Figure 6.20: Results: Accelerometer-06- Whole body vibration evaluation parameters: Blue bar-test and Red bar-sim

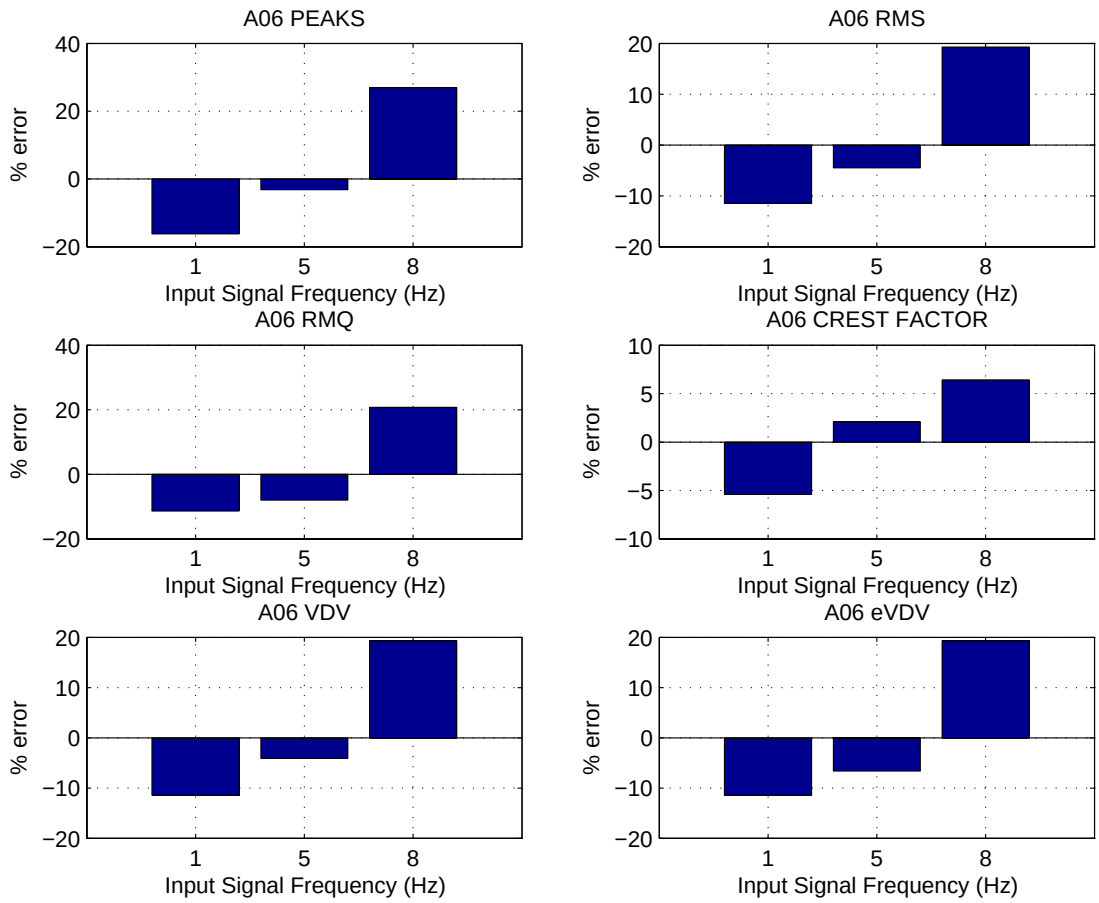

Figure 6.21: Results: Accelerometer-06-%*error* in the whole body vibration evaluation parameters

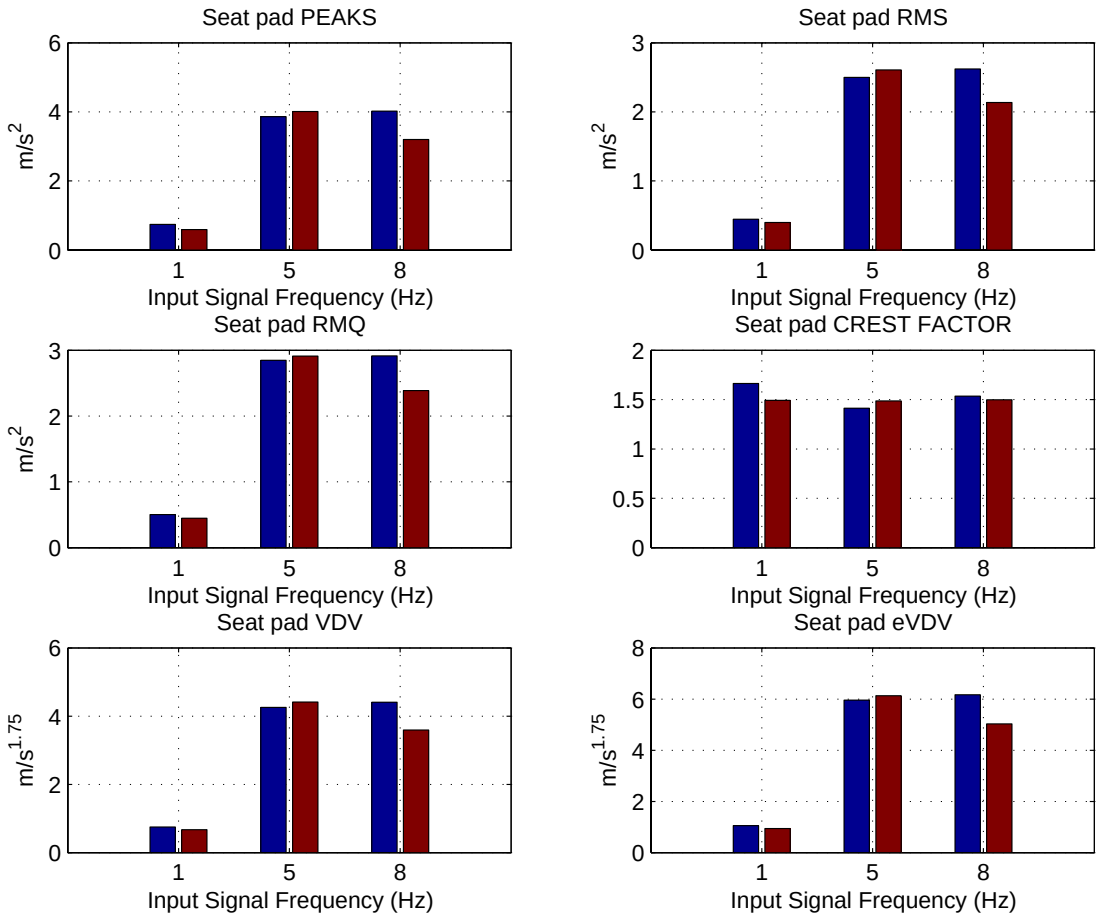

Figure 6.22: Results: Accelerometer-Seatpad- Whole body vibration evaluation parameters: Blue bar-test and Red bar-sim

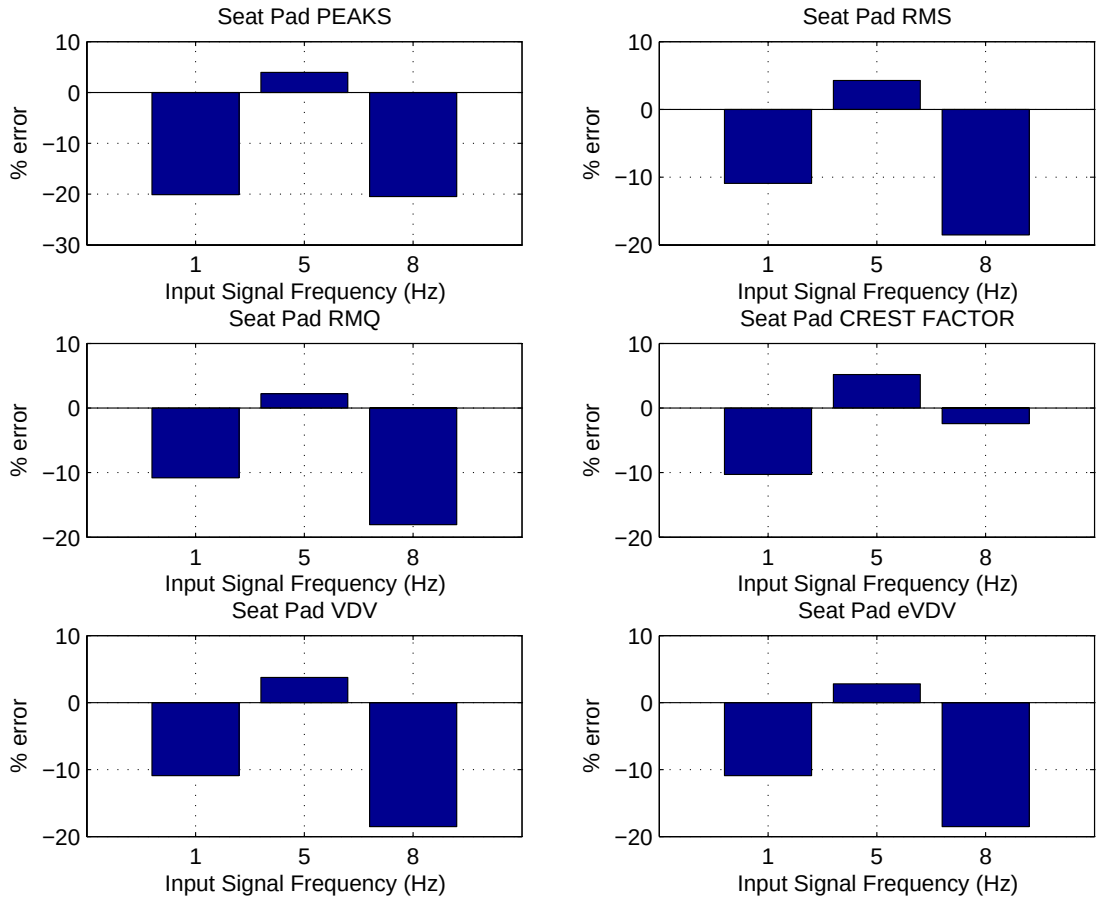

Figure 6.23: Results: Seatpad- $\%error$ in the whole body vibration evaluation parameters

printed on the right side of the plots. Figures 6.26 and 6.27 provide the corresponding plots in the frequency domain.

From the frequency domain plots in Figure 6.26 and 6.27 it can be observed that the model behavior is in a good agreement with the tested prototype in the 5hz region. As the input signal frequency increases the model deviates from the tested values. To quantify the model's performance from the point of view of whole body vibration parameters of peaks, rms, rmq,crest factor, VDV and eVDV the %*Accuracy* of the simulated and tested values is provided in Table 6.1 and 6.2. The accuracy values in Tables 6.1 and 6.2 although not within ideal accuracy limits, do present a good estimate of the level of vibration inputs to the dummy weight (human occupant).

Table 6.1: Accelerometer 06: %*Accuracy* of whole body vibration evaluation parameteres for random input signal

Parameter	**Test**	**Sim**	**Accuracy**
Peak	4.98	5.34	92.8%
RMS	1.35	1.14	84.5%
RMQ	1.88	1.53	82.5%
Crest	3.66	4.66	73%
VDV	2.87	2.41	84%
eVDV	4.02	3.38	85%

Table 6.2: Accelerometer Seatpad: %*Accuracy* of whole body vibration evaluation parameteres for random input signal

Parameter	**Test**	**Sim**	**Accuracy**
Peak	4.64	3.93	85%
RMS	1.3	1.01	78%
RMQ	1.77	1.35	77%
Crest	3.57	3.86	92%
VDV	2.75	2.15	79%
eVDV	3.85	3.01	79%

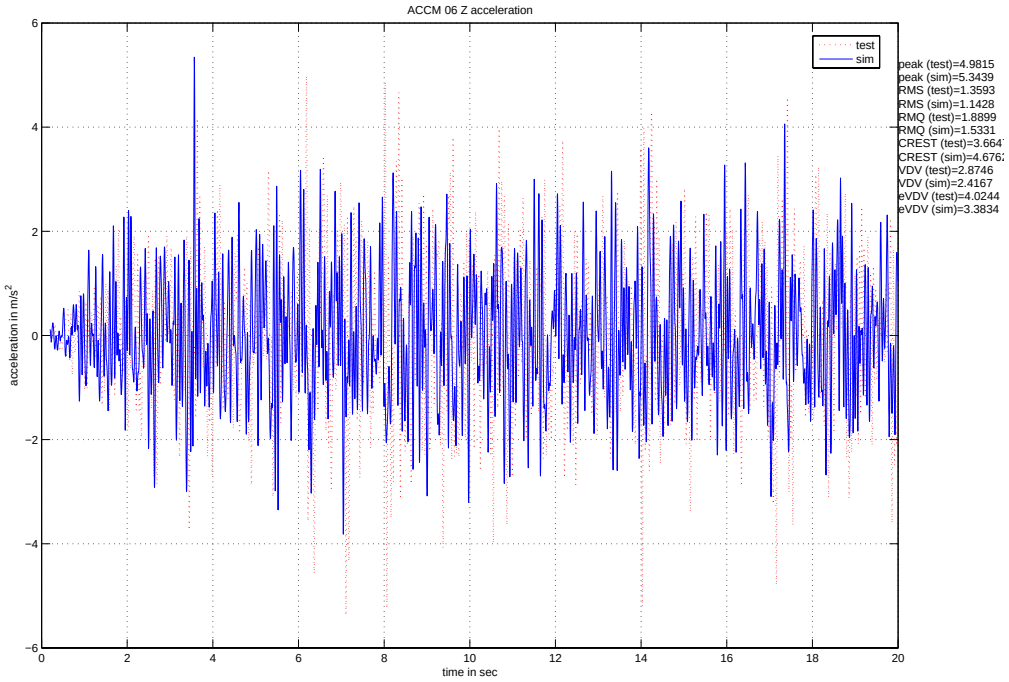

Figure 6.24: Results: Accelerometer-06 Z Random 0.5-20hz time plot

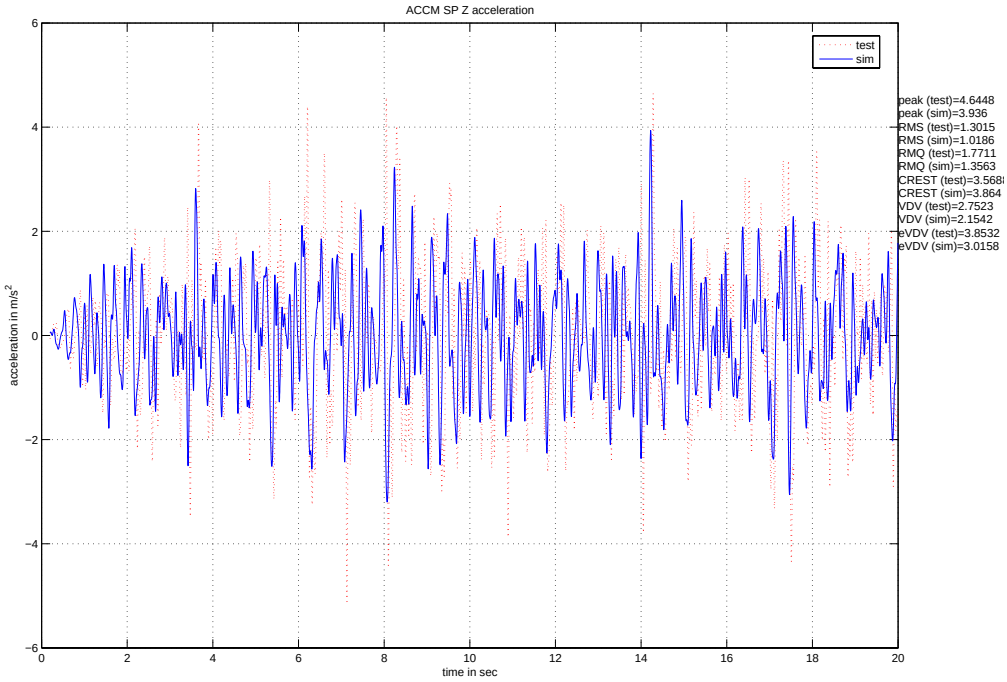

Figure 6.25: Results: Accelerometer-SP Z Random 0.5-20hz time plot

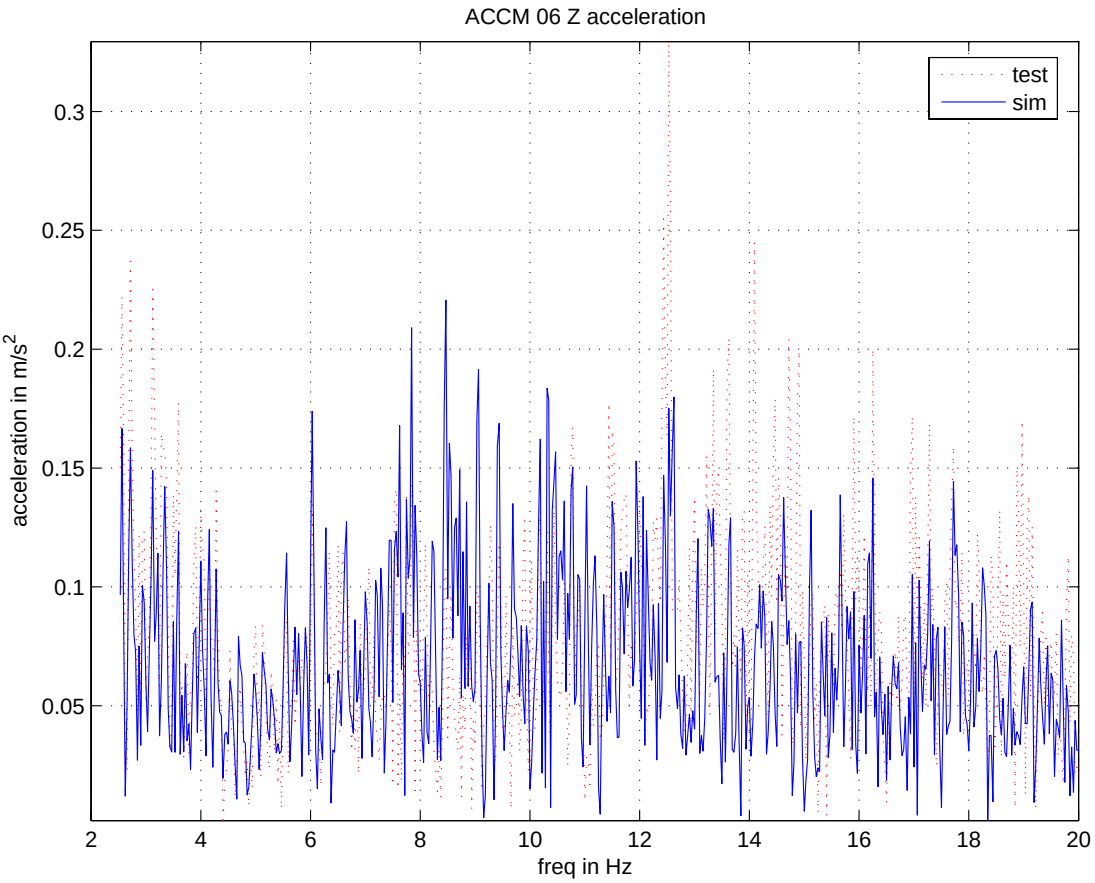

Figure 6.26: Results: Accelerometer-06 Z Random 0.5-20hz fft plot

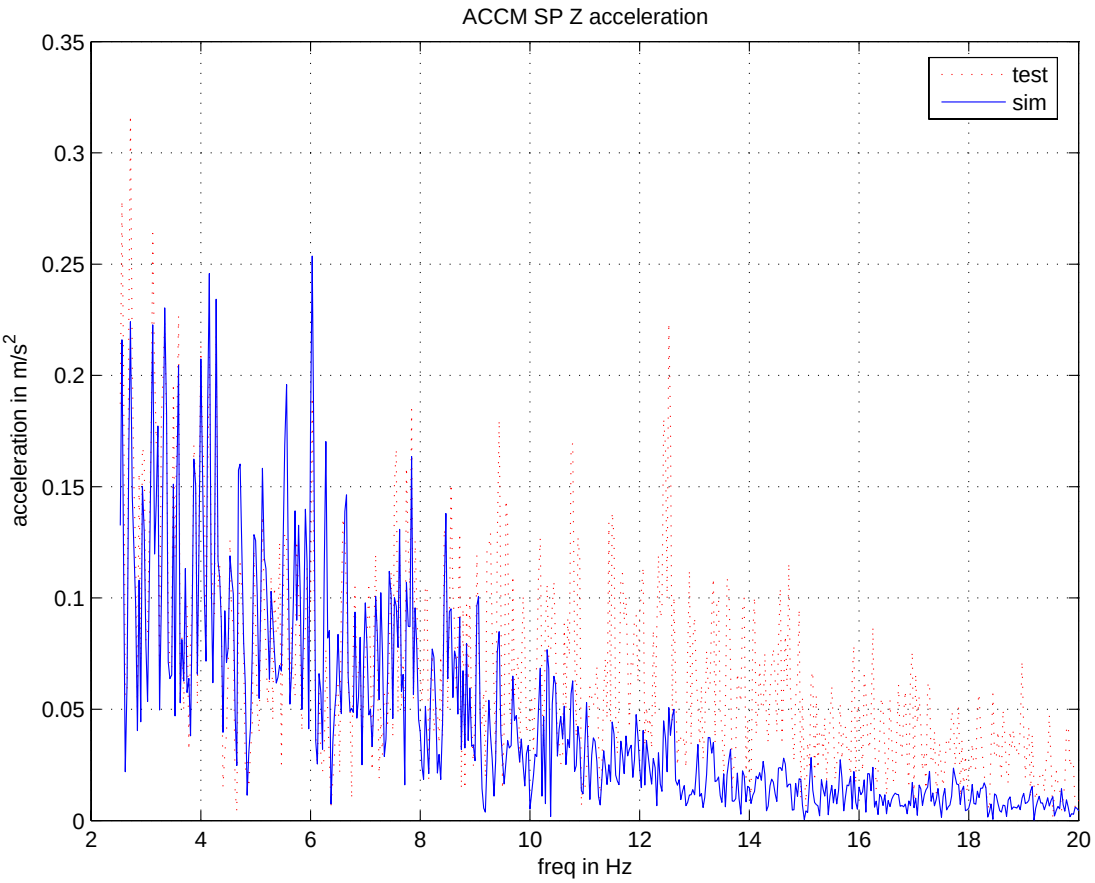

Figure 6.27: Results: Accelerometer-SP Z Random 0.5-20hz fft plot

Chapter 7

Conclusion and Future Work

This chapter discusses the conclusions of this thesis based on the results and observations in Chapter 6. Moreover, the degree of success achieved by this study with respect to the objectives is evaluated. The chapter concludes by listing the limitations of the model and providing the direction for future efforts.

7.1 Conclusion

The section is divided into two parts

- Part 1: discusses the conclusions for the MTS simulator model
- part 2: discusses the conclusions for the seat model

7.1.1 The MTS 6-Axis Simulator Model

The MTS simulator serves as the link between the real world vibration environment and the laboratory vibration environment for the seat. In the virtual world, the simulator model therefore has to ensure that the vibration input to the seat model matches the vibration input to the seat prototype tested. From Figures 6.1 to 6.6 it can be concluded that the simulator model's motion reproduction matches very closely, within 1.67x10^{-4}m, to that of the actual simulator, thus validating the model's use in virtual testing. Based on the approach used to verify the simulator model as mentioned in section 4.1, the agreement between the measured and simulated displacements at the actuator also validates the data processing methods, mainly the filtering and numerical integration. With the simulator model and data processing methods validated, the seat's vibration behavior can now be assessed.

7.1.2 The Seat Model

The following conclusions can be drawn for the seat model:

1. For the sinusoidal input (1Hz-8Hz), Figures 6.8 to 6.19 show that the model responds predictably to steady-state input. Even though the magnitude peaks for the simulations do not match the tested values exactly, the frequencies at which the peaks (first resonance)occur do match. This implies that the setup of the underlying mathematical model is correct. Figures 6.20 to 6.23 show that the system has a better accuracy in the 5Hz frequency zone as compared to either lower or higher frequencies. This can be attributed to the modeling approach used for the seat cushion and the airspring. The seat cushion was modeled using a transfer function, which is a linear element, while in reality the foam stiffness and damping are highly nonlinear and frequency dependent. The system identification was performed to give better accuracy in the 5Hz frequency region. The modeling of the airspring force was accurate, as seen from Figure 6.7, however the internal damping was modeled using a viscous damper whose value was again estimated at 5 Hz.

2. The response to random inputs as presented in section 6.3.2 further confirms the conclusion mentioned above. From Figures 6.26 and 6.27 it is evident that the model's vibration response matches closely in the 4-5Hz region, but as the frequency increases the deviation of the model's response from the prototype goes on increasing. The model limitations that attempt to explain this observation are discussed in section 7.2.

3. The virtual model, although not very accurate in predicting the absolute magnitude peaks in the FFT plots, is very useful in picking up behavioral trends as depicted by Figures 7.1 and 7.2, which are modified versions of Figures 6.26 and 6.27. It can be seen from Figure 7.1 that, the primary suspension attenuates the acceleration amplitudes in the 4-6Hz frequency range, thus satisfying the design need. However,Figure 7.2 shows that the seat cushion characteristics actually amplify the accelerations around the 5-6Hz region. Therefore, the models response to this random input (0.5-20Hz) brings out the design shortcoming, that although the seat suspension design is good by itself, the combination of the suspension parameters and the existing seat cushion is not the ideal one.

4. Figures 6.20 to 6.23 and Tables 6.1 , 6.2 hint towards the feasibility of the model's use in whole body vibration evaluations. From the sinusoidal response it can be concluded, although the model is not accurate in the entire range from 1-8Hz it has an accuracy of 95% at the crucial 5Hz frequency zone. The analysis of whole body

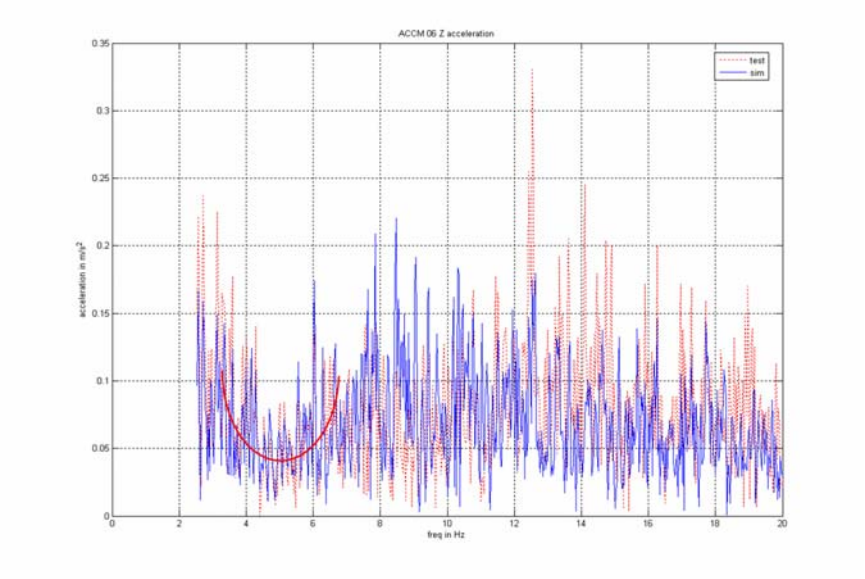

Figure 7.1: Suspension behavior highlighted by the simulated and measured response

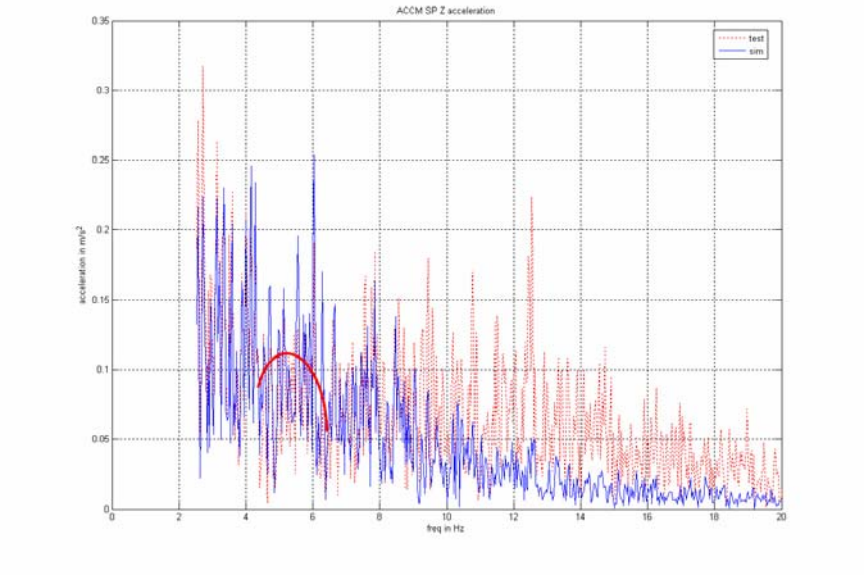

Figure 7.2: Seat cushion behavior highlighted by the simulated and measured response

vibration parameters for the random input gives accuracy values of approximately 75-85%. These are not in the ideal 95% or better region, however are useful to generate useful insights regarding the vibration exposure of the seat's occupant.

Thus it can be concluded that, the virtual model developed in this study is certainly feasible for use in the overall design process, though with the current modeling approach its accuracy is limited around the 5Hz frequency zone. The use of the model for whole body vibration evaluation also looks promising. This virtual model can therefore be a good starting point for design development and vibration analysis of prototypes. Subsequent improvements in the model, using a more detailed component level testing approach for addressing the nonlinearities would greatly improve the frequency range over which its response would be accurate.

7.2 Model Limitations

The model's deviation from the measured response in the higher frequency range can be mainly attributed to inability of the model to address the increasing contribution of non-linearities in the overall response. The main limitations of the model are

- The model is a rigid multibody dynamic model and so the vibration modes arising from the bending of the components like the suspension mechanism and the seat frame cannot be accounted for.
- All the joints are idealized and so do not take into account the impact arising from the play in real joints. This is especially important for the roller bearing sliding joints where there is always a clearance between the guide channels and the rollers.
- The seat cushion is modeled using a transfer function which is a linear element, while the foam properties are highly nonlinear and frequency dependent. This limitation is evident from the heavy attenuation of the acceleration levels through the seat cushion at higher frequencies, which is typical of a linear system (Figure 6.19).
- In the model, the dummy weight is constrained to move only in the vertical direction with the transfer function controlling the movement along the z-direction. However, in the real system the dummy weight is sitting on an infinite number of points over the surface of the cushion. The weight can rock and pivot in response to x,y,z motions. These rocking and pivoting actions give rise to acceleration peaks measured by the seat pad accelerometer as it lies exactly under the weight. These peaks cannot be reproduced by the constrained motion in the model.

These limitations provide the direction for the future work on the model.

7.3 Future Work

The main areas of improvements for future work are

- Seat cushion modeling: During the simulation runs and tuning exercises the seat cushion was observed to play a major role in the dynamic behavior of the seat. A more detailed component level approach needs to be undertaken for modeling the seat cushion properties.
- Flexible suspension components: The flexing of the suspension mechanism and the seat frame can be incorporated into the model using ADAMS/Flex. ADAMS/Flex can import FEM data from commercial FE software and overlay the FE information on the rigid components transforming them into flexible elements.
- Contact Modeling: 3-D contact can be modeled using CAD surfaces like the roller and the channel pairs in place of idealized joints, like the point-on-curve joints used to model the channel-roller pair in this model.
- Field data for model tuning: For tuning the model to address a wider frequency range, more realistic field data can be used in place of the computer generated random signals.

These improvements potentially can widen the frequency range over which, the model response can be considered as valid.

Bibliography

Bibliography

[1] James W. Dally, William F. Riley, and Kenneth G. McConnell. *Instrumentation for Engineering Measurements*. John Wiley and Sons, INC, second edition edition, 1984.

[2] Martin Fritz, Siegfried Fischer, and Peter Brode. Vibration induced low back disorder-comparison of the vibration evaluation according to iso 2631 with a force-related evaluation. *Applied Ergonomics*, pages 481–488, 2005.

[3] J. W. Frymore and M. H. Pope. The role of trauma in low back pain: A review. *Journal of Trauma*, pages 628–634, 1978.

[4] M. J. Griffin. *Handbook of Human Vibrations*. ELSEVIER Aacademic Press, London, 1990.

[5] Thomas Gunston. Annen d. the development of a suspension seat dynamic model.

[6] Cyril M. Harris. *Shock and Vibration Handbook*. McGraw-Hill Book Company, third edition edition, 1988.

[7] http://www.roymech.co.uk/useful tables/Tribology/co of friction. Coefficient of friction.

[8] kazuhito kato, Satoshi Kitazaki, and Hideo Tobata. Prediction of seat vibration with a seated human subject using a substructure synthesis method. *SAE Technical Paper Series*, SP-1877, 2004.

[9] Naresh Khude. Modal analysis of a helicopter wing-pylon structure using flexible multibody dynamics. Master's thesis, University of Tennessee, Knoxville, 2006.

[10] Chul kim and Paul I. Ro. An accurate full car ride model using model reducing techniques. *Journal of Mechanical Design*, 124:697–705, December 2002.

[11] Satoshi Kitazaki and Michael J. Griffn. Resonance behaviour of the seated human body and effects of posture. *Journal of Biomechanics*, pages 143–149, 1998.

[12] S. Kitazki and M. J. Griffin. A modal analysis of the whole-body vertical vibrations, using a finite element model of the human body. *Journal of Sound and Vibration*, pages 83–103, 1997.

[13] Sarah K. Leming and Harold L. Stalford. Bridge weigh-in-motion system development using superposition of dynamic truck/static bridge interaction. In *Proceedings of IMAC-XX;A conference of structural dynamics*, Los Angeles, CA, June 2002.

[14] Sarah K. Leming and Harold L. Stalford. Bridge weigh-in-motion system development using superposition of dynamic truck/static bridge interaction. In *Proceedings of the American Control Conference*, Denver,Colorado, June 2003. Sandia National Laboratories/University of Oklahoma.

[15] The Mathworks. *MATLAB Help*, matlab r14 2004 edition.

[16] MSC. Software. *ADAMS/View help*, adams/view 2005r2 edition.

[17] Katsuhiko Ogata. *System Dynamics*. Prentice Hall, fourth edition edition, 2003.

[18] M. M. Panjabi, G. B. J. Anderson, L. Jorneus, E. Hult, and L. Mattsson. Invivo measurements of spinal column vibrations. *Journal of Bone and Joint Surgery*, pages 695–702, 1986.

[19] D. E. Roberts and N. C. Hay. Dynamic response simulation through system identification. *Journel of Sound and Vibration*, pages 1017–1027, 2006.

[20] Jacob Rosen and Mircea Arcan. Modeling of human body/seat system in a vibration environment. *Journal of Biomechanical Engineering*, pages 223–231, 2003.

[21] Andrew Smyth and Meiliang Wu. Multi-rate kalman filtering for the data fusion of displacement and acceleration response measurements in dynamic system monitoring. *Mechanical Systems and Signal Processing*, 124:706–723, 2006.

Vita

Devdutt Shende was born in the city of Pune, India on August 17, 1981. He completed his high school as well as undergraduate education in Pune, receiving his Bachelor of Engineering - Mechanical degree from the University of Pune in August 2003. He became the first to take up engineering in his family of mostly commerce background. He then worked for one and a half years as a Design Engineer at Tata Motor's Engineering Research Center, India's leading vehicle manufacturer.

In Fall of 2005, he moved to the United States to pursue graduate education, at the University of Tennessee, Knoxville. He received his Masters of Science in Mechanical Engineering in Fall 2007.